Journal of Medicinal Chemistry Article

J. Med. Chem. **2009,** *52,* 6297–6313 **6297**
DOI: 10.1021/jm900526h

Synthesis and Structure−Activity Relationships of Cyanoguanidine-Type and Structurally Related Histamine H_4 Receptor Agonists[§]

Patrick Igel,[†] Roland Geyer,[†] Andrea Strasser,[†] Stefan Dove,[†] Roland Seifert,[‡] and Armin Buschauer*,[†]

[†]*Department of Pharmaceutical/Medicinal Chemistry, Faculty of Chemistry and Pharmacy, University of Regensburg, Universitatsstrasse 31, D-93053 Regensburg, Germany, and* [‡]*Institute of Pharmacology, Medical School of Hannover, D-30625 Hannover, Germany*

Received April 24, 2009

Recently, we identified high-affinity human histamine H_3 (hH_3R) and H_4 receptor (hH_4R) ligands among a series of N^G-acylated imidazolylpropylguanidines, which were originally designed as histamine H_2 receptor (H_2R) agonists. Aiming at selectivity for hH_4R, the acylguanidine group was replaced with related moieties. Within a series of cyanoguanidines, 2-cyano-1-[4-(1*H*-imidazol-4-yl)butyl]-3-[(2-phenylthio)ethyl]guanidine (UR-PI376, **67**) was identified as the most potent hH_4R agonist ($pEC_{50} = 7.47$, $\alpha = 0.93$) showing negligible hH_1R and hH_2R activities and significant selectivity over the hH_3R ($pK_B = 6.00$, $\alpha = -0.28$), as determined in steady-state GTPase assays using membrane preparations of hH_xR-expressing Sf9 cells. In contrast to previously described selective H_4R agonists, this compound and other 3-substituted derivatives are devoid of agonistic activity at the other HR subtypes. Modeling of the binding mode of **67** suggests that the cyanoguanidine moiety forms charge-assisted hydrogen bonds not only with the conserved Asp-94 but also with the hH_4R-specific Arg-341 residue. 2-Carbamoyl-1-[2-(1*H*-imidazol-4-yl)ethyl]-3-(3-phenylpropyl)guanidine (UR-PI97, **88**) was unexpectedly identified as a highly potent and selective hH_3R inverse agonist ($pK_B = 8.42$, >300-fold selectivity over the other HR subtypes).

Introduction

Histamine is a biogenic amine that influences a variety of physiological and pathophysiological processes in the body via stimulation of four histamine receptor (HR) subtypes, all belonging to the class A of G-protein-coupled receptors.[1,2] H_1R[a] and H_2R antagonists have been successfully used for several decades in the treatment of allergic conditions and as antiulcer drugs, respectively. The H_3R is mainly expressed in the CNS and acts as a presynaptic auto- or heteroreceptor modulating the release of several neurotransmitters.[3] This subtype has attracted interest as a potential drug target for the treatment of CNS disorders like attention-deficit hyperactivity disorder, Alzheimer's disease, Parkinson's disease, sleep disorders, or obesity.[4] Meanwhile, several H_3R antagonists, such as tiprolisant,[7] have been evaluated in the first clinical trials.[4]

The most recently identified fourth HR subtype, H_4R, was discovered on the basis of its high sequence homology with the H_3R in the years 2000 and 2001 independently by several research groups.[5−12] The H_4R is mainly expressed on hematopoietic cells such as mast cells, basophils, eosinophils, T-cells, and dendritic cells.[5,7,8,12−15] Up to now, little is known about the biological functions of the H_4R. Mast cell chemotaxis and calcium mobilization[14] as well as actin polymerization, shape change, expression of adhesion proteins, and chemotaxis of eosinophils are activated through this HR subtype.[16] Furthermore, the release of inflammatory mediators such as interleukin-16,[13] leukotriene-B_4,[17] and chemokine ligand 2[18] is modulated via the H_4R. In addition to such in vitro experiments, several animal models were used to evaluate the role of the H_4R. Blocking the H_4R with antagonists had protective effects in the mouse zymosan-induced peritonitis model[19] and in carrageenan-induced paw edemas in rats[20,21] and decreased lung inflammation in an asthma mouse model.[22] Moreover, the H_4R antagonist **1** (JNJ 7777120, Figure 1)[23] proved to be more effective in attenuation of pruritus than classic H_1R antagonists.[24]

The localization of the H_4R on immune cells and the in vitro and in vivo findings suggest that the receptor plays a crucial role in immunological and inflammatory processes. Hence,

[§] Dedicated to Prof. Dr. Helmut Schonenberger, University Regensburg, on the occasion of his 85th birthday.

*To whom correspondence should be addressed. Phone: +49-941 9434827. Fax: +49-941 9434820. E-mail: armin.buschauer@chemie.uni-regensburg.de.

[a] Abbreviations: α, intrinsic activity; aq, aqueous; Boc, *tert*-butyloxycarbonyl; Cbz, benzyloxycarbonyl; CDI, 1,1′-carbonyldiimidazole; DCM, dichloromethane; DMF, dimethylformamide; DMSO, dimethyl sulfoxide; EDTA, ethylenediaminetetraacetic acid; EI-MS, electron-impact ionization mass spectrometry; ES-MS, electrospray ionization mass spectrometry; GTP, guanosine 5′-triphosphate; GPCR, G-protein-coupled receptor; $G_{\beta 1\gamma 2}$, G protein β_1- and γ_2-subunit; $G_{\alpha i}$, α-subunit of the G_i protein that mediates inhibition of adenylyl cyclase; HMBC, heteronuclear multiple bond correlation; H_1R, histamine H_1 receptor; H_2R, histamine H_2 receptor; H_3R, histamine H_3 receptor; H_4R, histamine H_4 receptor; hH_1R, human H_1R; hH_2R, human H_2R; hH_2R-$G_{s\alpha S}$, fusion protein of the hH_2R and the short splice variant of $G_{s\alpha}$; hH_3R, human H_3R; hH_4R, human H_4R; hH_4R-RGS19, fusion protein of hH_4R and RGS19; HR-MS, high resolution mass spectrometry; HSQC, heteronuclear single quantum coherence; LSI-MS, liquid secondary ion mass spectrometry; NOESY, nuclear Overhauser enhancement spectrometry; RGS, regulator of G protein signaling proteins; SEM, standard error of the mean; TM, transmembrane domain of a GPCR; TFA, trifluoroacetic acid; THF, tetrahydrofuran.

Published on Web 09/30/2009

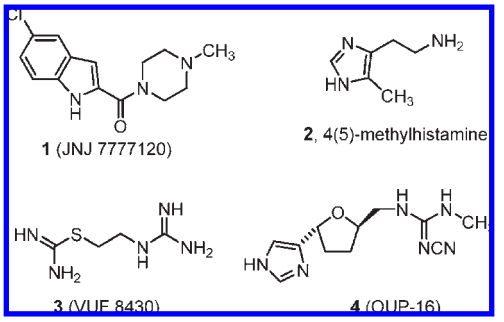

Figure 1. Structural formulas of the H_4R antagonist **1** and the selective H_4R agonists **2**, **3**, and **4**.

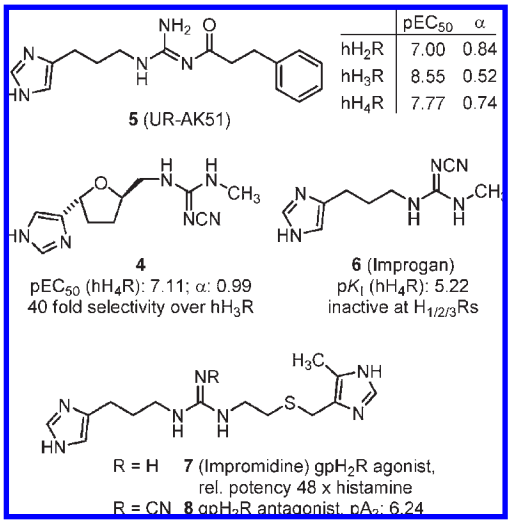

Figure 2. Imidazolylalkylguanidine derivatives reported as histamine receptor ligands.

the H_4R may be a promising drug target for the treatment of inflammatory and autoimmune diseases like allergic rhinitis, rheumatoid arthritis, bronchial asthma, and pruritus.[25] To further explore the biological function of this receptor, pharmacological tools (including selective agonists) are required.

Among the HR subtypes, the H_4R shows the highest degree of homology with the H_3R. Therefore, it is not surprising that many H_3R ligands also exhibit high affinity for the H_4R.[26] In particular for imidazole-based compounds such as thioperamide (*N*-cyclohexyl-4-(1*H*-imidazol-4-yl)piperidine-1-carbothioamide)[27] or proxyfan (5-[3-(benzyloxy)propyl]-1*H*-imidazole)[28] an overlap of H_3R- and H_4R-related effects is observed.[26] Only a limited number of selective H_4R agonists, including **2**, 4(5)-methylhistamine),[26] **3** (VUF 8430),[29] and **4** (OUP-16),[30] have been reported so far. However, these compounds have limitations because, at least at higher concentrations, they also activate other HR subtypes.

First approaches to the design of new selective H_4R agonists were based on N^G-acylated imidazolylpropylguanidines, originally developed as potent H_2R agonists.[31−33] More detailed pharmacological investigations revealed that several of these compounds are also active at the H_3R and H_4R. For example, compound **5** (UR-AK51)[32] is highly potent at both the H_3R and H_4R but exhibits lower efficacy at the H_3R relative to the H_4R (Figure 2). Very recently, we reported that imidazolylpropylguanidines bearing small N^G-acyl substituents show preference for H_4R and H_3R and considerably improved selectivity for the H_4R versus the H_2R.[34,35] With the

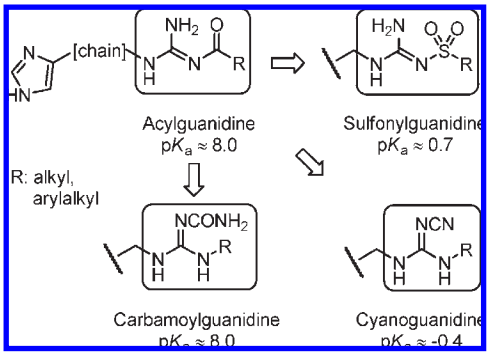

Figure 3. Replacement of the central acylguanidine group with a nonbasic cyanoguanidine or sulfonylguanidine group and a basic carbamoylguanidine group.

aim to further increase selectivity for the H_4R relative to the H_2R and H_3R, the present study was focused on the replacement of the acylguanidine moiety. Unlike the N^G-acylated imidazolylpropylguanidines ($pK_a \approx 8$),[36] the first reported selective H_4R agonist, compound **4**,[30] contains a nonbasic cyanoguanidine moiety ($pK_a \approx -0.4$).[37] Obviously, for H_4R activation a second basic component besides the imidazole ring is not essential. In contrast, when the strongly basic guanidine group in the potent H_2R agonist impromidine (**7**) is replaced, H_2R agonistic activity is abolished (Figure 2).[38] The antinociceptive drug improgan (**6**) (also containing a cyanoguanidine moiety) displays low affinity for the H_4R and lacks affinity for other HRs.[7] Moreover, in a series of thiourea-type H_3R antagonists, compounds with partial agonistic activity at the H_4R were identified[26] and the thiourea moiety is considered as a bioisostere of the cyanoguanidine group.[37] Therefore, cyanoguanidine analogues of the N^G-acylated imidazolylpropylguanidines[31−34,39] were prepared with the goal to obtain compounds that still exhibit agonistic activity at the H_4R but are devoid of agonistic activity at other HR subtypes. Besides the cyanoguanidines, several compounds were synthesized containing a carbamoylguanidine ($pK_a \approx 8.0$)[37] or a sulfonylguanidine ($pK_a \approx 0.7$)[36] moiety instead of the acylguanidine group (Figure 3), since central groups with different basicities may provide more insight into the structure−activity relationships at the distinct HR subtypes.

In this study the development of a new class of potent and selective hH_4R agonists and the unexpected discovery of a highly potent and selective carbamoylguanidine-type hH_3R inverse agonist are reported.

Chemistry

The cyanoguanidines **48**−**84**, **86**, and **87** and were synthesized by analogy to a previously described synthetic route (Scheme 1).[40] Aminolysis of diphenyl cyanocarbonimidate (**9**)[41,42] with the primary amines **10**−**26** at ambient temperature gave the isourea intermediates **27**−**43** that crystallized from diethyl ether. Conversion of the isoureas to the cyanoguanidines was performed by refluxing with histamine (**44**) or the analogous primary amines **45**−**47** or **85** in acetonitrile. Acidic hydrolysis of the cyanoguanidines resulted in the carbamoylguanidines **88**−**91**.[37]

The sulfonylguanidines **94** and **95** were prepared employing two different synthetic pathways (Scheme 2). **94** was synthesized by reaction of imidazolylpropylguanidine **88**[31] with tosyl chloride (**90**) followed by detritylation under acidic

Scheme 1. Synthesis of the Isourea Precursors **27**−**43**, the Cyanoguanidines **48**−**84**, **86**, and **87**, and the Carbamoylguanidines **88**−**91**[a]

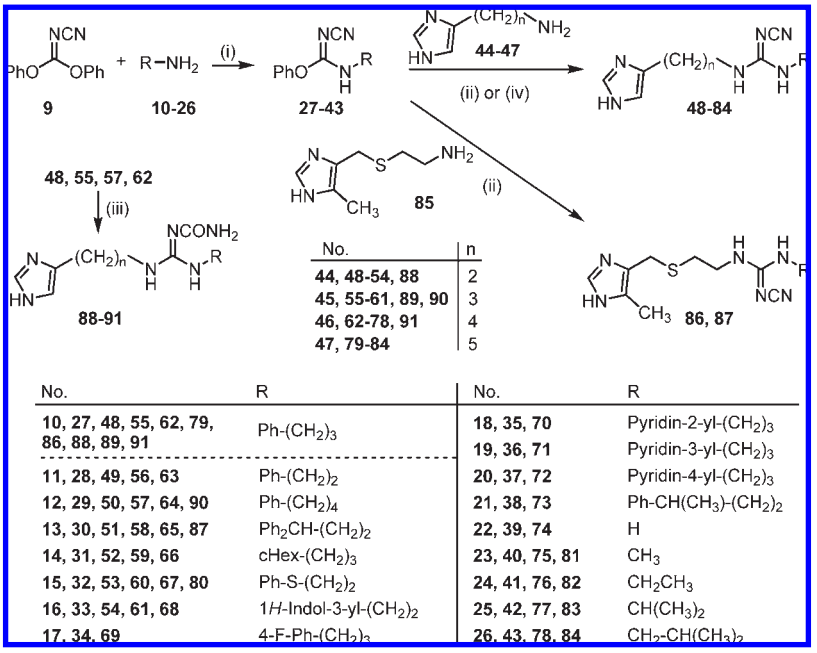

[a] Reagents and conditions: (i) DCM, 1 h, room temp; (ii) for **48**−**78**, MeCN, reflux, overnight; (iii) HCl 1 M, 14 days, room temp; (iv) for **79**−**84**, MeCN, microwave, 140 °C, 15 min.

Scheme 2. Synthesis of the N^G-Sulfonated Imidazolylpropylguanidines **94** and **95**[a]

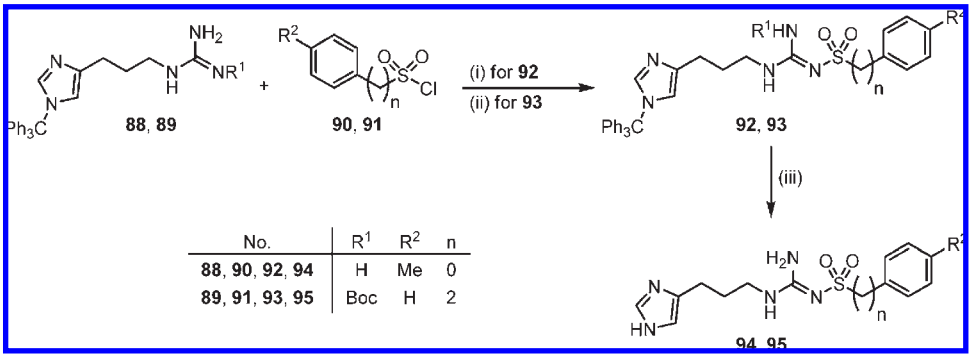

[a] Reagents and conditions: (i) NaH (60% dispersion in mineral oil) (2 equiv), NEt_3 (2 equiv), THF, overnight, 0 °C → room temp; (ii) DIEA (3 equiv), THF, overnight, 0 °C → room temp; (iii) TFA (20%), DCM, 5 h, room temp.

conditions. As several attempts to prepare **95** in the same manner failed, **88** was replaced with the less basic *tert*-butoxycarbonyl (Boc) protected analogue **89**. This method had already been successfully employed for the preparation of N^G-acylated imidazolylpropylguanidines[34] and turned out to be also appropriate for the preparation of **95**.

Results and Discussion

The prepared compounds were investigated for agonism and antagonism at the four hHR subtypes in steady-state GTPase assays measuring the enzymatic hydrolysis of radiolabeled GTP ([γ-^{32}P]GTP) by the G-protein coupled to the respective HR subtype. These experiments were performed using membrane preparations of Sf9 insect cells coexpressing the hH_1R plus RGS4, expressing the hH_2R-$G_{s\alpha S}$ fusion protein, coexpressing the hH_3R plus $G_{i\alpha 2}$ plus $G_{\beta 1\gamma 2}$ plus RGS4, or coexpressing the hH_4R-RGS19 fusion protein plus $G_{i\alpha 2}$ plus $G_{\beta 1\gamma 2}$ (Tables 1−5).[31,43,44] The major advantage of the well-proven test systems applied in this and in our previous studies is that an identical, very proximal read-out in G-protein-mediated signaling is used for any given HR subtype, namely, steady-state GTP hydrolysis. This read-out avoids bias in data interpretation caused by limited availability of downstream effectors.

Cyanoguanidines 48−84, 86, and 87 (Tables 1−4). Simple replacement of the acylguanidine moiety in **5** with a cyanoguanidine group should evaluate if this modification is tolerated by the hH_4R with respect to agonistic activity. Indeed, the resulting compound **55** showed partial agonism at the hH_4R (pEC_{50} = 6.12, α = 0.53). Moreover, **55** was almost inactive at the hH_1R and exhibited only weak partial agonism at the hH_2R (pEC_{50} = 4.85, α = 0.39). At the hH_3R, **55** behaved as a moderate inverse agonist (pK_B = 5.72, α = −0.37). However, compared to the reference compound **5** (hH_4R: pEC_{50} = 7.77, α = 0.74), efficacy and in particular potency at the hH_4R drastically decreased (almost 50-fold). With the aim of improving H_4R agonist potency, the phenylpropyl portion was varied. Similar residues as in the above-mentioned series of N^G-acylated

Table 1. Potencies and Efficacies of the Prepared Cyanoguanidine-Type Compounds **48**−**54** at the hH_1R, hH_2R, hH_3R, and hH_4R in the Steady-State GTPase Assay[a]

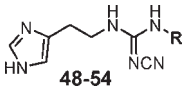

48-54

compound	R	hH_1R		hH_2R		hH_3R		hH_4R	
		$pEC_{50}/(pK_B)$	N	$pEC_{50}/(pK_B)$	N	$pEC_{50}/(pK_B)$	N	$pEC_{50}/(pK_B)$	N
Histamine		6.72[33] *α: 1.00*		5.92[33] *α: 1.00*		7.60 ± 0.05 *α: 1.00*	3	7.92 ± 0.09 *α: 1.00*	8
Thioperamide		-		-		7.01 ± 0.08 *α: -0.71 ± 0.06*		6.96 ± 0.06 *α: -0.95 ± 0.07*	6
4(5)-Methyl-histamine		4.80 ± 0.01 *α: 0.90 ± 0.02*	3	5.54 ± 0.18 *α: 1.01 ± 0.03*	4	[b]	3	7.15 ± 0.11 *α: 0.90 ± 0.06*	5
48	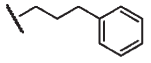	(< 5.00)	2	< 5.00	2	(5.18 ± 0.05) *α: -0.31 ± 0.02*	2	(< 5.00)	2
49	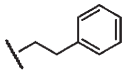	n.d.		inactive	1	n.d.		(5.18 ± 0.07) *α: 0.23 ± 0.05*	3
50	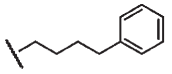	n.d.		(< 5.00)	1	n.d.		(< 5.00)	4
51	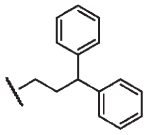	n.d.		(< 5.00)	3	n.d.		(< 5.00)	1
52	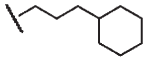	n.d.		5.41 ± 0.13 *α: 0.14 ± 0.01*	2	n.d.		(5.57 ± 0.07) *α: -0.23 ± 0.06*	3
53	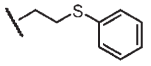	n.d.		(< 5.00)	1	n.d.		(5.05 ± 0.17) *α: -0.04 ± 0.09*	2
54	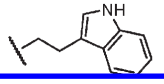	n.d.		(< 5.00)	1	n.d.		(< 5.00)	1

[a] Steady-state GTPase activity in Sf9 insect cell membranes expressing the hH_1R + RGS4, hH_2R-$G_{s\alpha S}$ fusion protein, $hH_3R + G_{i\alpha 2} + G_{\beta 1\gamma 2}$ + RGS4, or hH_4R-RGS19 fusion protein + $G_{i\alpha 2} + G_{\beta 1\gamma 2}$ was determined as described under Pharmacological Methods. *N* gives the number of independent experiments performed in duplicate each. n.d.: not determined. [b] No agonistic activity up to a concentration of 1 mM.

imidazolylpropylguanidines were introduced, since most of these compounds turned out to be potent hH_4R (partial)-agonists.[31] Shortening (**56**) and elongation (**57**) of the carbon chain resulted in considerably reduced potencies and efficacies. The branched diphenylpropyl residue in **58** caused a complete loss of activity, and replacement of phenyl with cyclohexyl (**59**) and 1*H*-indol-3-yl (**61**) eliminated hH_4R agonism ($\alpha = -0.20$ and -0.01, respectively). Only the imidazolylpropylcyanoguanidine **60**, bearing a phenylthioethyl substituent, retained some degree of hH_4R agonistic activity ($pEC_{50} = 5.89$, $\alpha = 0.33$).

Since the hH_4R agonistic potency could not be increased by modifying the N-substituent of **55**, attention was paid to optimization of the carbon chain connecting the imidazole ring with the cyanoguanidine group. This connecting chain proved to be critical for hH_4R agonism. The lower homologues of **55**−**61**, compounds **48**−**54** (Table 1), were substantially less potent and in all cases hH_4R antagonists. For instance, **48** was almost inactive ($pK_B < 5.00$) compared to **55**. By contrast, increasing the chain length in order to obtain higher similarity with the potent hH_4R agonist **4**[30] turned out to be a key step in structural optimization. The higher homologue of **55** (**62**) showed 5-fold higher potency and essentially improved intrinsic activity at the hH_4R ($pEC_{50} = 6.82$, $\alpha = 0.90$). As expected from the impromidine analogue **8**[38] (Figure 2), **62** exhibited only low potency and no significant efficacy at the hH_2R ($pEC_{50} = 5.25$, $\alpha = 0.08$). Furthermore, **62** was found to be almost inactive at the hH_1R ($pK_B < 5.00$) and only poorly active at the hH_3R ($pK_B = 5.64$, $\alpha = -0.03$). Notably, **62** is a potent and selective hH_4R agonist devoid of agonistic activity at the other HRs. Further elongation to a five-membered carbon chain in the compounds **79**−**84** (Table 4) was not tolerated with respect to hH_4R agonism. Independent from the second alkyl substituent, moderately potent hH_4R antagonists were obtained.

On the basis of these results, **62** was used as new lead structure to further improve hH_4R agonistic potency and selectivity. Keeping the imidazolylbutyl portion constant, structural modifications were again focused on the

Table 2. Potencies and Efficacies of the Prepared Cyanoguanidine-Type Compounds **55**−**61** at the hH_2R, hH_3R, and hH_4R in the Steady-State GTPase Assay[a]

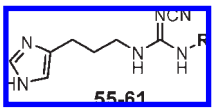

55-61

compound	R	hH_2R		hH_3R		hH_4R	
		$pEC_{50}/(pK_B)$	N	$pEC_{50}/(pK_B)$	N	$pEC_{50}/(pK_B)$	N
55	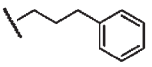	4.85 ± 0.03 *α: 0.39 ± 0.01*	2	(5.72 ± 0.08) *α: -0.37 ± 0.01*	2	6.12 ± 0.14 *α: 0.53 ± 0.06*	3
56	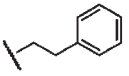	inactive	1	n.d.		(5.32 ± 0.31) *α: 0.13 ± 0.08*	2
57	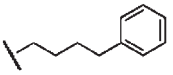	5.05 ± 0.13 *α: 0.17 ± 0.01*	2	n.d.		(5.22 ± 0.05) *α: -0.15 ± 0.03*	3
58	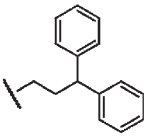	(< 5.00)	2	n.d.		(< 5.00)	3
59	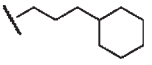	(< 5.00)	1	n.d.		(5.82 ± 0.03) *α: -0.20 ± 0.01*	2
60	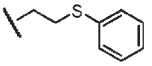	5.14 ± 0.08 *α: 0.57 ± 0.02*	2	n.d.		5.89 ± 0.18 *α: 0.33 ± 0.05*	2
61	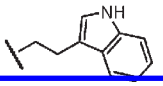	inactive	1	n.d.		(5.37 ± 0.08) *α: -0.01 ± 0.09*	2

[a] Steady-state GTPase activity in Sf9 insect cell membranes expressing the hH_2R-$G_{s\alpha S}$ fusion protein, hH_3R + $G_{i\alpha 2}$ + $G_{\beta 1\gamma 2}$ + RGS4, or hH_4R-RGS19 fusion protein + $G_{i\alpha 2}$ + $G_{\beta 1\gamma 2}$ was determined as described under Pharmacological Methods. *N* gives the number of independent experiments performed in duplicate each. n.d.: not determined.

substituent "R" of the cyanoguanidine-type compounds. Besides the residues employed in the homohistamine (**55**−**61**, Table 2) and histamine (**48**−**54**, Table 1) series, additional groups were introduced. Modifying the carbon spacer between the phenyl ring and the cyanoguanidine group was found to be critical. Reducing the chain length by only one methylene group (**63**) clearly reduced potency and efficacy (pEC_{50} = 5.96, α = 0.36). Elongation of the spacer (**64**) even caused a loss of efficacy (α = 0.05). Apparently, a definite distance between the cyanoguanidine moiety and the phenyl ring is required for hH_4R activation. Additionally, steric effects play a role. A bulky diphenylpropyl residue (**65**) generated a weak inverse agonist at the hH_4R (pK_B = 5.60, α = −0.43). By contrast, a methyl group in α-position to the phenyl ring (**73**) had no significant influence on potency and efficacy compared to **62** (pEC_{50} = 6.85, α = 0.79). Replacing the phenyl with a more bulky cyclohexyl (**66**) or indole ring (**68**) was not tolerated in terms of hH_4R activity. Notably, **68** was 10-fold more potent than **62** at the hH_3R (pK_B = 6.77). Surprisingly, a fluorine substituent in position 4 of the phenyl ring (**69**) was found to abolish hH_4R agonistic efficacy (pK_B = 6.59, α = −0.10). Replacement of the phenyl with a 2-, 3-, or 4-pyridyl ring (**70**−**72**) also resulted in lower potencies and efficacies at the hH_4R compared to **62**. Interestingly, potencies decreased in the rank order from the 2-pyridyl to the 4-pyridyl analogue (pEC_{50} = 6.24 → pEC_{50} = 5.59). In contrast, bioisosteric replacement of a methylene group in the connecting chain with a sulfur atom (**67**, UR-PI376) afforded a considerable increase in potency and retained high efficacy at the hH_4R (pEC_{50} = 7.47, α = 0.93) relative to compound **62**. It is noted that species-dependent discrepancies between affinities and potencies are reported for numerous H_4R ligands.[26,45,46] Since preliminary investigations revealed a substantially lower potency of compound **67** at the murine H_4R,[47] more detailed investigations on this aspect are the subject of ongoing work. At the hH_3R, **67** showed no agonism but moderate inverse agonistic activity (pK_B = 6.00, α = −0.30), and the (antagonistic) effects of **67** at the hH_1R and hH_2R were negligible (pK_B < 5.00).

Thus minor structural modifications of "R" in the imidazolylbutylcyanoguanidines can drastically change potency and efficacy. Since small alkyl substituents have already been successfully applied in a series of acylguanidine-type compounds to improve potency and intrinsic activity at the hH_4R,[34] a number of analogues bearing small alkyl residues (**75**−**78**, Table 3) as well as the unsubstituted parent compound (**74**) were prepared. Omitting the substituent (**74**) was well tolerated with respect to hH_4R agonistic activity. **74** was essentially equipotent and equiefficacious with **62** (pEC_{50} = 6.77, α = 0.91). However, compound **74** possessed similar potency at the hH_3R and, in contrast to the other

Table 3. Potencies and Efficacies of the Prepared Cyanoguanidine-Type Compounds **62**−**78** at the hH_1R, hH_2R, hH_3R, and hH_4R in the Steady-State GTPase Assay[a]

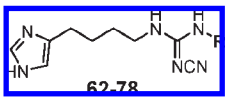

62-78

compound	R	hH_1R		hH_2R		hH_3R		hH_4R	
		$pEC_{50}/(pK_B)$	N	$pEC_{50}/(pK_B)$	N	$pEC_{50}/(pK_B)$	N	$pEC_{50}/(pK_B)$	N
62	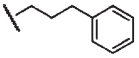	(< 5.00)	3	(5.25 ± 0.07) *α: 0.08 ± 0.05*	3	(5.64 ± 0.09) *α: -0.03 ± 0.06*	2	6.82 ± 0.14 *α: 0.90 ± 0.11*	3
63	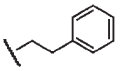	n.d.		(< 5.00)	3	(5.82 ± 0.05) *α: -0.23 ± 0.00*	2	5.96 ± 0.28 *α: 0.36 ± 0.05*	2
64	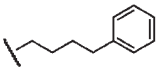	n.d.		(5.03 ± 0.01) *α: 0.11 ± 0.01*	2	(5.54 ± 0..07) *α: -0.13 ± 0.04*	2	(6.34 ± 0.04) *α: 0.05 ± 0.01*	2
65	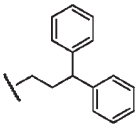	n.d.		(< 5.00)	2	n.d.		(5.60 ± 0.12) *α: -0,43 ± 0.11*	2
66	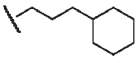	n.d.		(< 5.00)	2	(5.82 ± 0.10) *α: -0.21 ± 0.01*	2	(6.35 ± 0.02) *α: -0.15 ± 0.01*	2
67	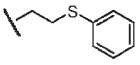	(< 5.00) *α: 0.07 ± 0.02*	2	(< 5.00) *α: 0.08 ± 0.01*	2	(6.00 ± 0.05) *α: -0.28 ± 0.02*	3	7.47 ± 0.01 *α: 0.93 ± 0.02*	3
68	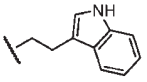	n.d.		(< 5.00) *α: 0.11 ± 0.02*	2	(6.77 ± 0.07) *α: -0.02 ± 0.02*	2	(5.80 ± 0.01) *α: -0.25 ± 0.05*	2
69	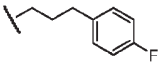	n.d.		(5.28 ± 0.01) *α: 0.17 ± 0.00*	2	(6.11 ± 0.06) *α: -0.28 ± 0.02*	2	(6.59 ± 0.01) *α: 0.10 ± 0.02*	2
70	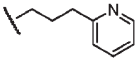	n.d.		(5.48 ± *0.03*) *α: 0.14 ± 0.01*	2	(5.89 ± 0.07) *α: -0.44 ± 0.01*	2	6.24 ± 0.10 *α: 0.57 ± 0.03*	2
71	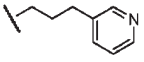	n.d.		(5.92 ± 0.04) *α: 0.15 ± 0.00*	2	(6.19 ± 0.02) *α: -0.13 ± 0.01*	2	5.92 ± 0.03 *α: 0.34 ± 0.04*	2
72	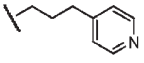	n.d.		(5.11 ± *0.12*) *α: 0.19 ± 0.00*	2	(6.11 ± 0.07) *α: -0.29 ± 0.00*	2	5.59 ± 0.05 *α: 0.42 ± 0.05*	2
73	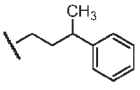	(< 5.00)	2	(< 5.00) *α: 0.16 ± 0.01*	2	(6.19 ± 0.01) *α: -0.29 ± 0.02*	2	6.85 ± 0.04 *α: 0.79 ± 0.03*	3
74		n.d.		(< 5.00) *α: 0.03 ± 0.00*	2	6.60 ± 0.11 *α: 0.42 ± 0.02*	2	6.77 ± 0.11 *α: 0.91 ± 0.00*	3
75		(< 5.00)	2	(< 5.00) *α: 0.03 ± 0.01*	2	(5.68 ± 0.14) *α: 0.16 ± 0.02*	2	6.02 ± 0.06 *α: 0.75 ± 0.03*	2
76		(< 5.00)	2	(< 5.00) *α: 0.05 ± 0.01*	2	(5.54 ± 0.09) *α: 0.09 ± 0.00*	2	6.15 ± 0.09 *α: 0.82 ± 0.01*	3
77		(< 5.00)	2	(< 5.00) *α: 0.07 ± 0.02*	2	(5.49 ± 0.07) *α: 0.07 ± 0.05*	2	6.48 ± 0.04 *α: 0.86 ± 0.02*	3
78	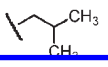	(< 5.00)	2	(< 5.00) *α: 0.07 ± 0.01*	2	(5.47 ± 0.13) *α: -0.05 ± 0.03*	2	6.92 ± 0.09 *α: 0.90 ± 0.02*	3

[a] Steady-state GTPase activity in Sf9 insect cell membranes expressing the hH_1R + RGS4, hH_2R-$G_{s\alpha S}$ fusion protein, hH_3R + $G_{i\alpha 2}$ + $G_{\beta 1\gamma 2}$ + RGS4, or hH_4R-RGS19 fusion protein + $G_{i\alpha 2}$ + $G_{\beta 1\gamma 2}$ was determined as described under Pharmacological Methods. *N* gives the number of independent experiments performed in duplicate each. n.d.: not determined.

Table 4. Potencies and Efficacies of the Prepared Cyanoguanidine-Type Compounds **79**−**84** at the hH_2R, hH_3R, and hH_4R in the Steady-State GTPase Assay[a]

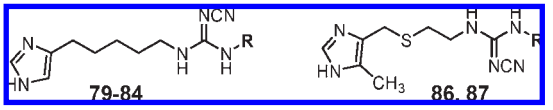

compound	R	hH_2R		hH_3R		hH_4R	
		$pEC_{50}/(pK_B)$	N	$pEC_{50}/(pK_B)$	N	$pEC_{50}/(pK_B)$	N
79	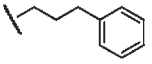	(5.28 ± 0.22)	2	(6.55 ± 0.05)	2	(6.96 ± 0.11) *α: -0.26*[b]	2
80	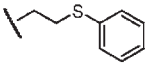	(5.21 ± 0.09)	2	(6.74 ± 0.02)	2	(6.85 ± 0.04) *α: 0.16*[b]	2
81		(5.66 ± 0.07)	2	(6.38 ± 0.09)	2	(6.54 ± 0.01) *α: 0.21*[b]	2
82		(5.37 ± 0.16)	2	(6.92 ± 0.02)	2	(6.47 ± 0.05) *α: -0.03*[b]	2
83		(5.57 ± 0.02)	2	(6.47 ± 0.19)	2	(6.25 ± 0.03) *α: 0.08*[b]	2
84	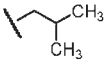	(< 5.00)	2	(6.57 ± 0.13)	2	(6.51 ± 0.10) *α: 0.04*[b]	2
86	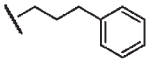	(5.74 ± 0.17) *α:* -0.15 ± 0.04	2	n.d.		(< 5.00)	2
87	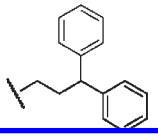	(5.80 ± 0.15) *α:* -0.11 ± 0.06	2	n.d.		(< 5.00)	2

[a] Steady-state GTPase activity in Sf9 insect cell membranes expressing the hH_2R-$G_{s\alpha S}$ fusion protein, hH_3R + $G_{i\alpha 2}$ + $G_{\beta 1\gamma 2}$ + RGS4, or hH_4R-RGS19 fusion protein + $G_{i\alpha 2}$ + $G_{\beta 1\gamma 2}$ was determined as described under Pharmacological Methods. *N* gives the number of independent experiments performed in duplicate each. n.d.: not determined. [b] $N = 1$.

imidazolylbutylcyanoguanidines, exhibited partial agonistic activity at this subtype (pEC_{50} = 6.60, α = 0.42). The substituent "R" appears to be indispensable to discriminate between the hH_3R and hH_4R. This assumption is supported by the data of the alkylated analogues **75**−**78**. Introduction of a methyl group (**75**) resulted in 10-fold lower potency at the hH_3R (pK_B = 5.68, α = 0.16) but also hH_4R potency decreased (pEC_{50} = 6.02, α = 0.75). However, enlarging the alkyl substituent increased potency at the hH_4R (Me < Et < *i*-Pr < *i*-Bu, pEC_{50} = 6.02 → pEC_{50} = 6.92) without remarkably affecting efficacy (α = 0.75−0.90). By contrast, at the hH_3R, with increasing alkyl residues partial agonistic activity was abolished whereas affinity was not markedly affected (pK_B = 5.68 → pK_B = 5.47). In conclusion, the pharmacological data show that larger alkyl substituents are required for high hH_4R potency and selectivity relative to the hH_3R. For example, an almost 30-fold selectivity in combination with high potency and efficacy at the hH_4R was achieved for compound **78**, characterized by a bulky isobutyl residue (pEC_{50} = 6.92, α = 0.90). The activities of **74**−**78** at the hH_1R and hH_2R were negligible (very weak antagonism, pK_B < 5.00).

Recently, 5-methylhistamine was identified as a selective hH_4R agonist.[26] Hence, two compounds (**86** and **87**, Table 4) bearing a methyl group at position 5 of the imidazole ring were prepared to evaluate if this modification can also improve selectivity of cyanoguanidine-type hH_4R agonists. Because of the availability of the corresponding amine, the prepared compounds contain a sulfur atom in the chain separating the imidazole ring from the cyanoguanidine group. Unfortunately, both synthesized compounds (**86** and **87**) including the analogue of the lead compound **62** were almost inactive at the hH_4R (no agonism; very weak antagonism, pK_B < 5.00).

The optimization steps from the acylguanidine-type compound **5** toward the potent and selective cyanoguanidine-type hH_4R agonist **67** are summarized in Figure 4 and the structure−activity relationships of the cyanoguanidines **48**−**84**, **86**, and **87** in Figure 5.

Carbamoylguanidines 88−**91 (Table 5).** Although potent and selective hH_4R agonists were obtained in the cyanoguanidine series, the potencies of these compounds at the hH_4R were lower than those of the corresponding acylguanidine-type compounds.[34] To study to which extent the lack of basicity of the cyanoguanidine group accounts for the differences in hH_4R potencies, some structurally related but basic carbamoylguanidine-type compounds were prepared (**88**−**91**; $pK_a \approx 8.0$).[37] By analogy to the cyanoguanidine series, compounds with a two- (**88**), three- (**89** and **90**), and four-membered (**91**) carbon chain separating the imidazole

Table 5. Potencies and Efficacies of the Prepared Carbamoylguanidine-Type Compounds **88**–**91** and Sulfonylguanidine-Type Compounds **94** and **95** at the hH_1R, hH_2R, hH_3R, and hH_4R in the Steady-State GTPase Assay[a]

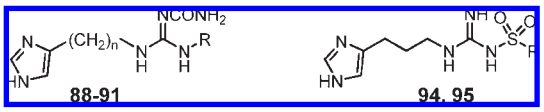

compound	R	n	hH_1R		hH_2R		hH_3R		hH_4R	
			$pEC_{50}/(pK_B)$	N	$pEC_{50}/(pK_B)$	N	$pEC_{50}/(pK_B)$	N	$pEC_{50}/(pK_B)$	N
88	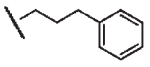	2	(< 5.00) *α: -0.02 ± 0.01*	3	5.70 ± 0.06 *α: 0.26 ± 0.01*	2	(8.42 ± 0.01) *α: -0.97 ± 0.04*	3	(5.89 ± 0.02) *α: -0.51 ± 0.02*	2
89	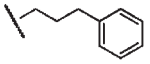	3	(< 5.00)	2	6.19 ± 0.02 *α: 0.65 ± 0.01*	2	(6.23 ± 0.07) *α: -0.67 ± 0.03*	2	(6.77 ± 0.03) *α: -0.75 ± 0.06*	2
90	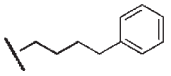	3	n.d.		6.42 ± 0.02 *α: 0.55 ± 0.01*	2	(6.51 ± 0.04) *α: -0.75 ± 0.02*	2	(6.33 ± 0.02) *α: -0.76 ± 0.03*	2
91	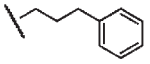	4	n.d.		6.36 ± 0.12 *α: 0.46 ± 0.01*	2	(6.44 ± 0.01) *α: -0.52 ± 0.01*	2	(7.07 ± 0.01) *α: -0.68 ± 0.06*	2
94	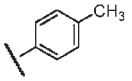	-	(< 5.00)	2	4.92 ± 0.03 *α: 0.47 ± 0.07*	2	(6.11 ± 0.03) *α: -0.33 ± 0.03*	2	(5.85 ± 0.11) *α: 0.26 ± 0.02*	2
95	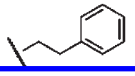	-	n.d.		4.92 ± 0.10 *α: 0.53 ± 0.04*	3	(6.57 ± 0.01) *α: -0.67 ± 0.02*	2	(5.85 ± 0.10) *α: -0.14 ± 0.08*	2

[a] Steady-state GTPase activity in Sf9 insect cell membranes expressing the hH_1R + RGS4, hH_2R-$G_{s\alpha S}$ fusion protein, $hH_3R + G_{i\alpha 2} + G_{\beta 1\gamma 2}$ + RGS4, or hH_4R-RGS19 fusion protein + $G_{i\alpha 2} + G_{\beta 1\gamma 2}$ was determined as described under Pharmacological Methods. *N* gives the number of independent experiments performed in duplicate each. n.d.: not determined.

ring from the carbamoylguanidine group were investigated for their pharmacological activities at the hHRs. In contrast to the cyanoguanidine **55** that showed partial agonistic activity at the hH_4R ($\alpha = 0.53$), the carbamoylguanidine analogue **89** exerted considerable inverse agonistic activity ($\alpha = -0.75$). Potency of **89** at the hH_4R was moderate ($pK_B = 6.77$). The phenylbutyl analogue **90** exhibited comparable potency and intrinsic activity. Like at the hH_4R, **89** and **90** were moderately potent inverse agonists at the hH_3R. Interestingly, both carbamoylguanidines showed moderate partial agonistic activity at hH_2R ($\alpha \approx 0.60$). As expected from **48**, the histamine analogue **88** (UR-PI97) exhibited weak inverse agonistic activity at the hH_4R ($pK_B = 5.89$, $\alpha = -0.51$). Analogous to **89** and **90**, **88** behaved as weak partial agonist at the hH_2R ($pEC_{50} = 5.70$, $\alpha = 0.26$) and showed negligible activity at the hH_1R ($pK_B < 5.00$). Surprisingly, this compound turned out to be a highly potent hH_3R inverse agonist ($pK_B = 8.42$, $\alpha = -0.97$). Compared to the cyanoguanidine analogue **48**, introduction of the carbamoylguanidine moiety resulted in a more than 1500-fold increase in potency. In addition, **88** is highly selective over the hH_1R, hH_2R, and hH_4R (>2500-fold, > 500-fold, and >300-fold selectivity, respectively). The high selectivity of **88** relative to the hH_4R is not typical, as many imidazole containing H_3R ligands such as thioperamide or iodophenpropit (1-[3-(1*H*-imidazol-5-yl)propylthio]-*N*′-[2-(4-iodophenyl)ethyl]formamidine)[48] also have high affinity for the H_4R.[26] In the cyanoguanidine series highest hH_4R agonistic activity resided in compounds having a tetramethylene chain connecting the imidazole ring and the cyanoguanidine group. By contrast, the imidazolylbutylcarbamoylguanidine **91** showed no agonistic activity at the hH_4R and had similar pharmacological activities as the carbamoylguanidines **89** and **90** at the other HR subtypes.

Although the cyanoguanidine- and carbamoylguanidine-type compounds have closely related structures, the compounds have distinct pharmacological profiles. In contrast to the cyanoguanidines, the basicity of the carbamoylguanidines is sufficiently high to allow protonation under physiological conditions. However, the discrepancies in the pharmacological activities at the HRs cannot only be explained by differences in basicity. Ionic interactions with the conserved $Asp^{3.32}$ of TM3 that are crucial for histamine binding at all HR subtypes may be replaced by charge-assisted hydrogen bonds in the case of neutral groups. Obviously, variations in the bulk and the binding conformations of the central groups are the main reasons for the observed differences in HR subtype activity.

Sulfonylguanidines 94 and 95 (Table 5). Additional investigations were carried out to evaluate the influence of the basicity on HR subtype activity and selectivity using the sulfonylguanidines **94** and **95**. Unlike the acylguanidine group ($pK_a \approx 8$),[36] the sulfonylguanidine group ($pK_a \approx 0.7$)[36] is virtually uncharged at physiological pH. The sulfonylguanidine analogue of **5**, **95**, showed a more than 50-fold decrease in potency at the hH_4R ($pK_B = 5.85$) and, contrary to **5**, had no agonistic activity. The same was observed for the sulfonylguanidine **94** (acylguanidine analogue at the hH_4R: $pEC_{50} = 8.21$, $\alpha = 0.40$). **94** and **95** acted as moderate inverse agonists at the hH_3R and showed partial agonism at the hH_2R ($\alpha \approx 0.50$). However, potencies were reduced by 2 orders of magnitude relative to the acylated guanidines at the

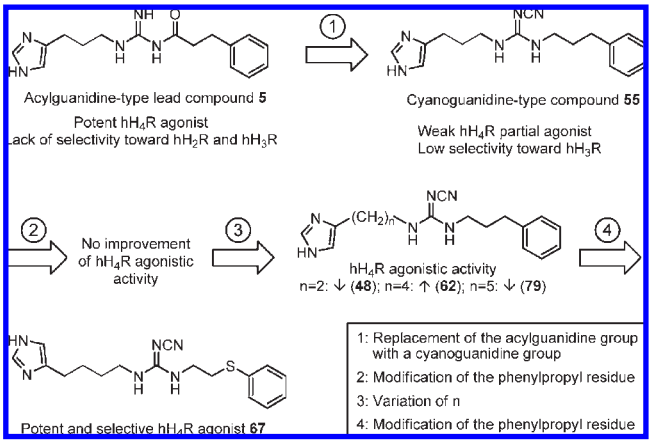

Figure 4. Optimization steps from the acylguanidine-type compound **5** toward the potent and selective cyanoguanidine-type hH_4R agonist **67**.

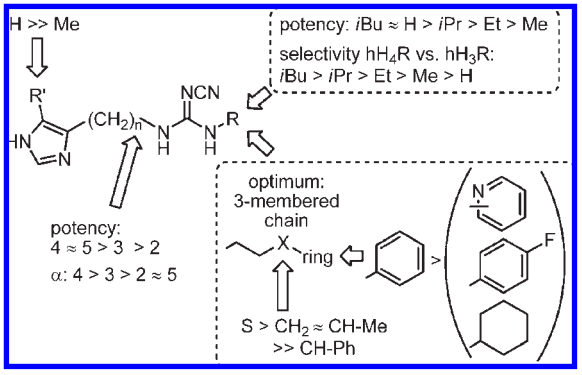

Figure 5. H_4R agonistic potency of the cyanoguanidines **48**−**84**, **86**, and **87**: summary of structure−activity relationships.

H_2R subtype (pEC_{50} = 4.92). Again, these findings do not indicate that basicity is a necessary condition for interaction with HR subtypes. Steric and electronic effects, as for example the different orientation of the oxygen atoms and the influence of the sulfonyl group on the conformation of the chain may play a role in altering the pharmacological activities.

Model of the hH_4R in Complex with Compound 67 and Other hH_4R Agonists. To explore the putative binding site of the cyanoguanidines, a homology model of the hH_4R was developed based on the crystal structures of the human β_2-adrenoceptor.[49,50] Compound **67** was manually docked in an energetically favorable conformation, considering results from in vitro mutagenesis[51] and modeling approaches.[52] Figure 6A,B shows the complex, minimized subsequent to MD simulations in a membrane environment (see Experimental Section). The cyanoguanidine moiety is presented as the "cyanoimine" tautomer which is, according to ab initio calculations,[53] about 12 kcal mol^{-1} lower in energy than the most favorable conformation of the "cyanoamine" tautomer. The given *Z* isomer may slowly topomerize at room temperature into the *E* configuration by inversion at the planar imine nitrogen (calculated topomerization barrier of ~23 kcal mol^{-1}).[54]

The binding site of compound **67**, consisting of 20 amino acids with side chains not more than 3 Å distant from the ligand, is located between TM 2 and TM 7. The imidazole moiety is docked as proposed by Jongejan et al.[52] and corresponding to results on hH_4R mutants. In this binding mode, Glu-$182^{5.46}$ is assumed to be protonated and serves as hydrogen bond donor for the π nitrogen. (Superscripts indicate the generic numbering scheme of amino acids in TMs 1−7 proposed by Ballesteros and Weinstein[55]). The τ nitrogen forms another H bond with the side chain oxygen of Thr-$178^{5.42}$. However, a similar bidentate interaction is possible with the couple Ser-$179^{5.43}$/Glu-$182^{5.46}$ if the imidazole ring is assumed to be coplanar with the butyl chain. Both the Thr-178 and the Ser-179 alanine mutations lead to an only 3- to 4-fold reduction of histamine affinity and potency.[51] Thus, no definitive conclusion about the presence and the partner of a second hydrogen bond can be drawn. The given mode is more likely, since a nearly perpendicular conformation of the imidazolyl ring with respect to an alkyl chain is energetically favorable and present in the crystal structure of histamine monohydrobromide, too.[56]

Figure 6C shows that the binding mode of the semirigid cyanoguanidine-type agonist **4** is very similar to that of compound **67**. The butyl chain of **67** aligns in a staggered conformation with the furanylmethyl spacer of **4**, leading to the same imidazole−guanidine distance of 6.0 Å and to closely corresponding positions of the imidazole and the cyanoguanidine moieties in both structures. A rather roomy binding pocket in the region of the spacer enables the fit of different folds and bulks. Interactions occur with Tyr-$95^{3.34}$, Cys-$98^{3.37}$, Trp-$316^{6.48}$, Tyr-$319^{6.51}$, and Phe-$344^{7.39}$. The inactivity of the 5-methylhistamine derivatives **86** and **87** may be due to sterical hindrance of the 5-methyl group by Tyr-$95^{3.34}$ or, in the case of interactions with the Ser-$179^{5.43}$/Glu-$182^{5.46}$ couple, by Tyr-$319^{6.51}$.

In both models (Figure 6B,C), the cyanoguanidine moiety is stacked with the phenyl ring of Phe-$344^{7.39}$ and forms two charge-assisted hydrogen bonds with the carboxylate oxygens of Asp-$94^{3.32}$ (distances 2.0−2.1 Å), an amino acid proven to be essential for histamine binding by in vitro mutagenesis.[51] This arrangement allows the arylthioalkyl substituent of compound **67** to point outward like the isopropyl group of carazolol in the crystal structure of the β_2-adrenoceptor.[49] In the given *Z* configuration, the cyano group forms two additional charge-assisted hydrogen bonds with the guanidine moiety of Arg-$341^{7.36}$ (distances 2.1−2.2 Å) which is also involved in a salt bridge with Glu-165 (E2). This arginine is species specific (rat and mouse H_4R: serine) and replaced by a glutamate in the hH_3R. Therefore, the suggested interactions with Arg-$341^{7.36}$ may contribute to the hH_4R subtype and species selectivity of the cyanoguanidines. Except His-$75^{2.64}$ (hH_3R, Tyr), Thr-$178^{5.42}$ (Ala), and Gln-$347^{7.42}$ (Leu), all other transmembrane amino acids of the binding site in Figure 6 are identical in hH_3R and hH_4R. Interestingly, the species selectivity of agonistic imidazolylpropylguanidines for the gpH_2R versus the hH_2R is also related to a mutation in position 7.36 (gpH_2R, Asp; hH_2R, Ala) as shown by in vitro mutagenesis.[43,57] For the carbamoyl derivatives representing inverse agonists at the hH_4R (Table 5), another binding mode of the central protonated guanidine moiety must be supposed. One reason is the additional bulk of the carbamoyl NH_2 group. Furthermore, the guanidinium cation may adopt another position with respect to Asp-$94^{3.32}$ by forming a salt bridge.

Also the considerably less potent imidazolylpropyl analogue of **67**, compound **60**, may form the suggested key interactions of the imidazole and the cyanoguanidine moiety

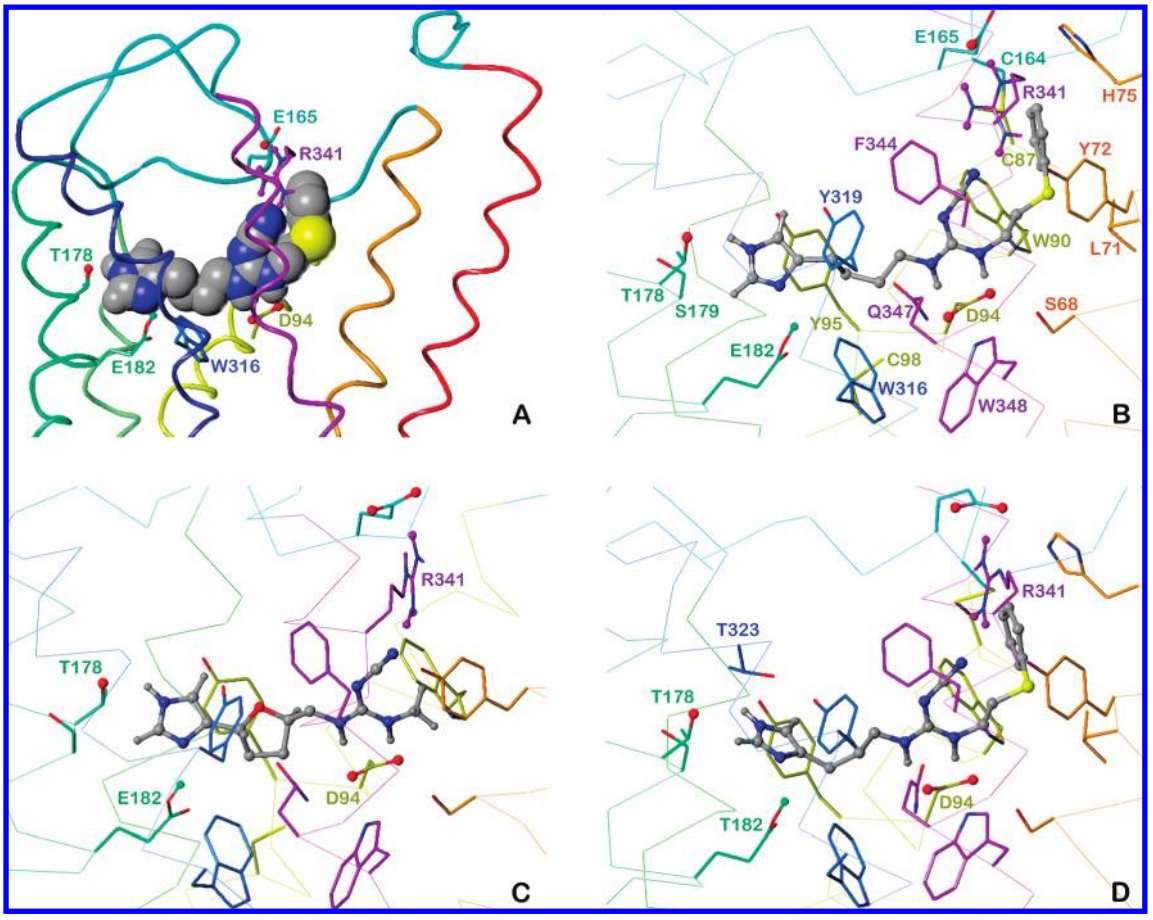

Figure 6. Model of the hH_4R binding site for the agonists **67**, **4**, and **60**. The backbone, C atoms, and some essential hydrogens of the amino acids are individually drawn in spectral colors: TM1, red; TM2, orange; TM3, yellow; TM4, green; E2, cyan; TM5, green−blue; TM6, blue; TM7, violet; nitrogens, blue; oxygens, red; sulfur, yellow; C and H atoms of the ligands, gray. (A) Space fill representation of compound **67** within a tube model of the backbone. Side chains probably forming key interactions with the cyanoguanidines are drawn as sticks, the interacting atoms as balls. (B−D) Detailed model of the binding modes of (B) compound **67**, (C) compound **4**, and (D) compound **60**. Drawn are the Cα trace (lines), Cα atoms, and side chains (sticks) of all amino acids within 3 Å around the ligands, and the ligands (balls and sticks). Atoms forming key interactions are marked as balls. For clarity of presentation, the labeling of amino acids in panels C and D is restricted to key and extra contacts.

with the hH_4R (Figure 6D). However, the conformational strain of the propyl spacer is higher than in the case of the butyl chain, and the guanidine is not ideally face to face with Asp-$94^{3.32}$. The position of the imidazole plane differs from that in compound **67** by ∼30°, leading to an additional weak contact with Thr-$323^{6.55}$. Taken together, the model in Figure 6D provides possible reasons for the lower potency of compound **60**.

The outstanding potency of compound **67** is probably due to the close fit of the phenylthioethyl substituent R into a predominantly hydrophobic binding pocket at the top of TMs 2 and 3 (Figure 6B), leading to interactions that may even compensate for the entropically and conformationally more favorable binding of compound **4**. The phenylthio moiety is surrounded by the side chains of Leu-$71^{2.60}$, Tyr-$72^{2.61}$, His-$75^{2.64}$, and Trp-$90^{3.28}$. In the model, this pocket is quite narrow, suggesting why even slight variations of the geometry and the bulk of R (phenylpropyl, **62**) reduce potency and why a cyclohexylpropyl group (inverse hH_4R agonist **66**) may not fit in the given binding mode. In contrast, it becomes obvious that small alkyl chains and methyl branches in α-, β-, and γ-position are well tolerated (**73**, **75**−**78**). For instance, the methyl group of **4** is centered to the π-plane of Tyr-$72^{2.61}$ (Figure 6C). In the case of a diphenylpropyl substituent (inverse hH_4R agonist **65**), the second phenyl group clashes with Tyr-$72^{2.61}$. Interestingly, this compound is inactive at the hH_2R, indicating that the binding mode of the cyanoguanidines at this subtype differs from that proposed for corresponding H_2R agonistic N^G acylated imidazolylpropylguanidines.[31] In this mode, diphenylpropyl groups are favorable, since the hH_2R contains a serine in position 2.61 which provides enough space to accommodate the second aryl moiety into a binding pocket between TM 2 and TM 7.

The model in Figure 6 does not directly explain why *p*-F substitution changes the agonism of **62** into antagonism (compound **69**). Also, the hH_4R antagonist **64**, the phenylbutyl analogue of **67**, may principally form the key interactions of the imidazole and the cyanoguanidine moiety with the receptor described above. However, docking approaches with **64** (not shown) indicate that the long phenylbutyl chain affects the conformation of E2, thereby possibly preventing the stabilization of the active state. Compound **69** may behave in a similar manner. Since a single amino acid in the E2 loop, Phe-169, seems to account for the differences in agonist binding between human and mouse H_4 receptors,[45] a

specific conformational change of E2 bringing Phe-169 close to the binding pocket could be necessary for the active state formation.

Taken together, the model shown in Figure 6, although based only on the putative inactive state of the receptor, provides some information about which amino acids and interactions could account for the hH_4R agonistic potency and selectivity of the cyanoguanidines. A reliable model of the fully active state cannot be obtained without appropriate crystal structures. However, the docking poses in Figure 6 contain direct contacts of the spacers with Trp-316$^{6.48}$ and interactions with Tyr-319$^{6.51}$ probably participating in correlated rotamer changes by which Trp-316$^{6.48}$ may serve as toggle switch, leading to subsequent modification of the proline kink in TM6.[58] A pocket of amino acids in TMs 6 and 7, consisting of Tyr-319$^{6.51}$, Phe-344$^{7.39}$ (in contact with the cyanoguanidine moiety and with Arg-341$^{7.36}$), Gln-347$^{7.42}$, and Trp-348$^{7.43}$, may contribute to the conformational change of Trp-316$^{6.48}$, suggesting that flexibility of TM7 could affect the toggle switch. Thus, hH_4R-selective potency and efficacy may indeed be due to specific interactions of the cyanoguanidines with TM7. Perhaps different conformations and flexibilities of the E2 loop[45] with individual transient interactions and energy gradients during binding may contribute to affinity, potency, efficacy, and selectivity.

Affinities of 67 for the hH_1R, hH_2R, hH_3R, and hH_4R Subtypes in Radioligand Binding Experiments. **67** was identified as the most potent and selective hH_4R agonist in the cyanoguanidine series by using steady-state GTPase assays (pEC_{50} = 7.46, α = 0.93, ~30-fold selectivity toward the hH_3R). Nevertheless, agonist potencies determined in functional assays depend on different factors such as receptor/G-protein stoichiometry, compartmentation of signaling proteins, and G-protein subtype.[33,59] This can cause discrepancies between potencies obtained in functional experiments and binding studies. For this reason inhibition constants (pK_I values) of **67** at the different hHR subtypes were determined. **67** displaced [^{3}H]mepyramine from the hH_1R, [^{3}H]tiotidine from the hH_2R, [^{3}H]N^{α}-methylhistamine from the hH_3R, and [^{3}H]histamine from the hH_4R, yielding monophasic competition binding isotherms (Figure 7). In accordance with the results from the GTPase assay, **67** bound with the highest affinity to the hH_4R (pK_I = 7.24) and, as expected, showed a remarkably lower affinity for the hH_3R (pK_I = 6.28). However, the affinity of **67** for the hH_4R was slightly reduced compared to the pEC_{50} value determined in the GTPase activity assay (pEC_{50} = 7.46), while the contrary was observed for the affinity of **67** to the hH_3R (pEC_{50} = 6.00). Therefore, selectivity of **67** for the hH_4R over the hH_3R is about 3 times lower than in the functional experiments. At the hH_1R and hH_2R, the compound displayed low affinity, resulting in a 450- and 70-fold selectivity for the hH_4R, respectively. Overall, the determined pK_I values and their rank orders are in agreement with the potencies evaluated in the functional GTPase assays and confirm **67** to be a high-affinity and selective ligand for the hH_4R.

Inhibition of the 67-Stimulated GTP Hydrolysis by Standard H_4R Antagonists. The functional pharmacological activities of all compounds were determined in steady-state GTPase activity assays using membrane preparations of Sf9 insect cells expressing the respective HR subtype. When membrane preparations are used instead of intact cells,

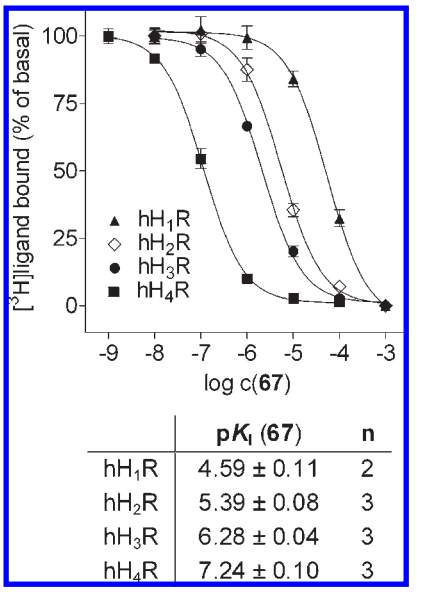

	pK_I (67)	n
hH_1R	4.59 ± 0.11	2
hH_2R	5.39 ± 0.08	3
hH_3R	6.28 ± 0.04	3
hH_4R	7.24 ± 0.10	3

Figure 7. Displacement of [^{3}H]mepyramine (5 nM), [^{3}H]tiotidine (10 nM), [^{3}H]N^{α}-methylhistamine (3 nM), and [^{3}H]histamine (10 nM) with **67** from Sf9 insect cell membranes expressing the hH_1R + RGS4, hH_2R-$G_{s\alpha S}$ fusion protein, hH_3R + $G_{i\alpha 2}$ + $G_{\beta 1\gamma 2}$ + RGS4, or hH_4R-RGS19 fusion protein + $G_{i\alpha 2}$ + $G_{\beta 1\gamma 2}$. Radioligand binding was determined as described under Pharmacological Methods. Data were analyzed for best fit to one site (monophasic) competition curves. Data points shown are the means values of *n* independent experiments each performed in duplicate.

G-proteins are directly accessible to the evaluated compounds. Therefore, the possibility of direct, receptor-independent G-protein activation has to be taken into account. For many compounds like the wasp venom mastoparan, local anesthetics, β-adrenoceptor antagonists, and cationic-amphiphilic HR ligands, direct G-protein activation has been reported.[60−62] **67** with its polar and basic imidazole ring and more lipophilic side chain possesses cationic−amphiphilic properties. To exclude a direct G-protein activation, GTPase activity was stimulated with **67** (1 μM) and the effect of increasing concentrations of the H_4R antagonists (inverse agonists) thioperamide, iodophenpropit, and **1** was evaluated. As shown in Figure 8, all compounds inhibited the **67**-induced GTP hydrolysis in a concentration-dependent manner. Thioperamide was more efficacious in suppressing GTP hydrolysis than the other standard H_4R ligands because of its pronounced inverse agonistic activity at the hH_4R (Table 1). The pK_B values determined for thioperamide, iodophenpropit, and **1** against **67** in the functional assay were in good accordance with pK_I values from binding studies reported in the literature (Figure 8). These results indicate the H_4R ligands to compete with **67** for the same binding site at the hH_4R and suggest the GTPase activation through **67** to be receptor-mediated. Direct G-protein activation by HR receptor ligands was reported to occur at > 10 μM.[60−62] By contrast, **67** stimulated GTPase activation in membranes expressing the hH_4R was detectable at ≥10 nM. The inverse agonistic activity of **67** at the hH_3R also supports a receptor-dependent effect, as both the hH_3R and hH_4R were coexpressed with $G_{i\alpha 2}$. Finally, **67** was found to displace [^{3}H]histamine from the hH_4R (Figure 7). These data confirm **67** to act as a hH_4R agonist in the GTPase assay, whereas direct G-protein stimulation can definitely be ruled out.

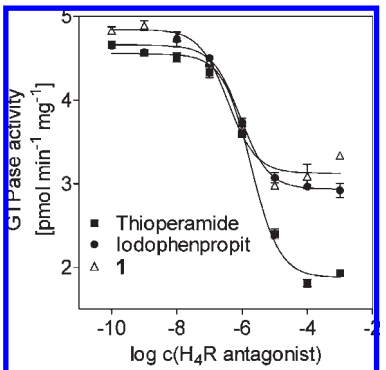

Compound	K_B [nM]	K_i [nM][a]
Thioperamide	62 ± 4.6	125
Iodophenpropit	30 ± 2.4	13
1	12 ± 2.5	16

Figure 8. Inhibition of the **67**-stimulated GTP hydrolysis at the hH_4R by the H_4R antagonists thioperamide, iodophenpropit, and **1**. Steady-state GTPase activity in Sf9 insect cell membranes expressing the hH_4R-RGS19 fusion protein + $G_{i\alpha 2}$ + $G_{\beta 1\gamma 2}$ was determined as described under Pharmacological Methods. Reaction mixtures contained 1 μM **67**. Data were analyzed by nonlinear regression and were best-fit to sigmoid concentration−response curves. Data points shown are the mean values of two independent experiments each performed in duplicate. Footnote "a" indicates from ref 26.

Summary and Conclusion

Starting from the N^G-acylated imidazolylpropylguanidine **5**, which is lacking HR subtype selectivity and shows high activities at $hH_{2/3/4}Rs$, several classes of compounds with structurally related polar central groups were prepared. The aim was to obtain potent hH_4R agonists with improved selectivity compared to **5** and information about structure−activity relationships of the compounds at the distinct HR subtypes.

Replacing the acylguanidine moiety in **5** with a cyanoguanidine group produced **55** that exhibited moderate partial agonism at the hH_4R. Altering the chain length between the imidazole ring and the cyanoguanidine group revealed a tetramethylene spacer to be optimal for high potency and efficacy at the hH_4R. By contrast, two- and five-membered carbon chains were not tolerated with respect to hH_4R agonism. The substituent "R" of the imidazolylbutylcyanoguanidines was found to be sensitive toward variations. Minor modifications, for example, altering the chain length or fluorine substitution of the phenyl ring, substantially reduced hH_4R activity. Introduction of small alkyl residues was well accepted, but larger substituents increased selectivity over the hH_3R. At the hH_1R and hH_2R, most cyanoguanidines showed negligible efficacies and just low potencies. Compared to the hH_1R and hH_2R, higher activities were observed for the hH_3R. Almost all imidazolylbutylcyanoguanidines were potent agonists or partial agonists at the hH_4R but were antagonists at the other hHR subtypes. Modeling of their binding mode suggests that the cyanoguanidine moiety forms charge-assisted hydrogen bonds not only with the conserved Asp-$94^{3.32}$ but also with the hH_4R-specific Arg-$341^{7.36}$ residue.

Exchange of the cyanoguanidine with a carbamoylguanidine group drastically changed the pharmacological activities at the HRs. All compounds displayed inverse agonistic activity at the hH_4R, whereas partial agonism was observed at the hH_2R. With **88** unexpectedly a new highly potent carbamoylguanidine-type hH_3R inverse agonist was discovered that is 25 times more potent than the standard H_3R ligand thioperamide. In contrast to thioperamide, which is essentially equipotent at the hH_3R and hH_4R, for **88**, a more than 300-fold selectivity over the hH_4R was found. Since many reported imidazole-type H_3R antagonists/inverse agonists also bind with high affinity to the H_4R,[26] **88** belongs to the most selective imidazole containing hH_3R inverse agonists known so far.

Furthermore, new potent and selective cyanoguanidine-type hH_4R agonists were obtained. **67** turned out to be the most potent hH_4R agonist in this series. Compared to the lead compound **5**, **67** is devoid of agonistic activities at the hH_2R and hH_3R, and the selectivity for the hH_4R toward the hH_2R and hH_3R subtype considerably increased (approximately 300- and 30-fold in the GTPase assay, respectively). In contrast to **67** other selective hH_4R agonists such as 5-methylhistamine[26] (Table 1), *S*-(2-guanidinoethyl)isothiourea,[29] or **4**[30] have agonistic activities at other HR subtypes. Moreover, **67** has negligible activity at the hH_1R whereas the hH_4R agonist clozapine shows more than 100-fold higher affinity for this histamine receptor subtype relative to the hH_4R.[26,63] Therefore, the new cyanoguanidine-type H_4R agonist **67** will be a valuable additional pharmacological tool to study the biological functions of the hH_4R.

Experimental Section

Chemistry. General Conditions. Commercial reagents and chemicals were purchased from Acros Organics (Geel, Belgium), IRIS Biotech GmbH (Marktredwitz, Germany), Alfa Aesar GmbH & Co. KG (Karlsruhe, Germany), Merck KGaA (Darmstadt, Germany), Sigma-Aldrich Chemie GmbH (Munich, Germany), TCI Europe (Zwijndrecht, Belgium) and used without further purification. Deuterated solvents for NMR spectroscopy were from Deutero GmbH (Kastellaun, Germany). All solvents were of analytical grade or distilled prior to use. If moisture-free conditions were required, reactions were performed in dried glassware under inert atmosphere (argon or nitrogen). Anhydrous DMF was purchased from Sigma-Aldrich Chemie GmbH. 3-(1-Trityl-1*H*-imidazol-4-yl)propan-1-ol (**96**) was a gift from Prof. Dr. Sigurd Elz, Department of Pharmaceutical/Medicinal Chemistry I, University of Regensburg. Flash chromatography was performed on silica gel (Merck silica gel 60, 40−63 μM). Reactions were monitored by TLC on aluminum plates coated with silica gel (Merck silica gel 60 F_{254}, thickness 0.2 mm). The compounds were detected by UV light (254 nm), a 0.3% solution of ninhydrine in *n*-butanol (amines), or a 1.0% solution of Fast Blue B salt (imidazole containing compounds) in $EtOH/H_2O = 30/70$ (v/v). All melting points are uncorrected and were measured on a Buchi 530 (Buchi GmbH, Essen, Germany) apparatus. Microwave assisted reactions were performed on an Initiator 2.0 synthesizer (Biotage, Uppsala, Sweden).

Nuclear magnetic resonance spectra (^{1}H NMR and ^{13}C NMR) were recorded with Bruker Avance 300 (^{1}H, 300.1 MHz; ^{13}C, 75.5 MHz), Avance 400 (^{1}H, 400.1 MHz; ^{13}C, 100.6 MHz) or Bruker Avance 600 (^{1}H, 600.1 MHz; ^{13}C, 150.9 MHz) NMR spectrometers (Bruker BioSpin GmbH, Rheinstetten, Germany). Chemical shifts are given in δ (ppm) relative to external standards. Abbreviations for the multiplicities of the signals are as follows: s (singlet), d (doublet), t (triplet), q (quartet), quin (quintet), sep (septet), m (multiplet), brs (for broad singlet), and combinations thereof. The multiplicity of carbon atoms (^{13}C NMR) was determined by DEPT 135 (distortionless enhancement by polarization transfer): "+",

primary and tertiary carbon atom (positive DEPT 135 signal); "−", secondary carbon atom (negative DEPT 135 signal); "quat", quaternary carbon atom. In certain cases 2D-NMR techniques (COSY, HMQC, HSQC, HMBC, NOESY) were used to assign ^{1}H and ^{13}C chemical shifts. Infrared spectra (IR) were measured on a Bruker Tensor 27 spectrometer equipped with an ATR (attenuated total reflection) unit from Harrick Scientific Products Inc. (Ossining, NY). Mass spectra (MS) were recorded on a Finnigan MAT 95 (EI-MS 70 eV, HR-MS), Finnigan SSQ 710A (CI-MS (NH_3)), or a Finnigan ThermoQuest TSQ 7000 (ES-MS) spectrometer. The peak intensity in % relative to the strongest signal is indicated in parentheses. Elemental analyses (C, H, N, Heraeus Elementar Vario EL III) were performed by the Analytical Department of the University Regensburg and are within ±0.4% unless otherwise noted.

Preparative HPLC was performed with a pump model K-1800 (Knauer, Berlin, Germany). The column was Eurosphere-100 (250 mm × 32 mm) (Knauer), which was attached to a UV detector model K-2000 (Knauer). UV detection of the compounds was done at 210 nm. The temperature was 25 °C and the flow rate 37 mL/min. The mobile phase was 0.1% TFA in Millipore water and MeCN. Analytical HPLC was performed on a system from Thermo Separation Products (TSP, Egelsbach, Germany) equipped with a SN 400 controller, P4000 pump, an AS3000 autosampler, and a Spectra Focus UV/vis detector. Stationary phase was a Eurosphere-100 C-18 (250 mm × 4.0 mm, 5 μm) column (Knauer) thermostatted at 30 °C. The flow rate was 0.8 mL/min, and the dead time (t_0) was 3.32 min. For some compounds analytical HPLC was performed on a Merck-Hitachi system equipped with a L-5000 LC controller, 655A-12 LC pump, a 655A-40 autosampler, and a L-4250 UV/vis detector. Stationary phase was a Eurosphere-100 C-18 (250 mm × 4.0 mm, 5 μm) column (Knauer) thermostatted at 25 °C. The flow rate was 0.7 mL/min, and the dead time (t_0) was 2.54 min. Mobile phase gradients of MeCN/0.05% TFA (aq) were used, and the absorbance was detected at 210 nm. Compound purities were calculated as the percentage peak area of the analyzed compound by UV detection at 210 nm. HPLC conditions, retention times (t_R), capacity factors ($k' = (t_R - t_0)/t_0$), and purities of the synthesized compounds are listed in the Supporting Information.

Preparation of the Isoureas 27−43. General Procedure. A solution of the pertinent primary amine (1 equiv) and diphenyl cyanocarbonimidate (**9**, 1 equiv) in DCM was stirred for 1 h. After evaporation of the solvent, the product was crystallized from Et_2O.

1-Cyano-2-phenyl-3-[2-(phenylthio)ethyl]isourea (32). The title compound was prepared from **15**[64] (1.53 g, 10.0 mmol) and **9** (2.38 g, 10.0 mmol) in DCM (50 mL) according to the general procedure, yielding a white solid (2.6 g, 86%); mp 110 °C. ^{1}H NMR (300 MHz, $CDCl_3$): δ [ppm] = 3.18 (t, 2H, ^3J = 7.0 Hz, Ph-S-C$\boldsymbol{H}_2$), 3.55−3.69 (m, 2H, Ph-S-CH$_2$-C$\boldsymbol{H}_2$), 7.05 (d, 2H, ^3J = 7.8 Hz, Ph-***H***), 7.15−7.50 (m, 8H, Ph-***H***), 7.57 (t, 1H, ^3J = 6.1 Hz, N-***H***). ^{13}C NMR (75 MHz, $CDCl_3$): δ [ppm] = 33.22 (−, Ph-S-***C***H$_2$), 41.68 (−, Ph-S-CH$_2$-***C***H$_2$), 115.55 (C$_{quat}$, ***C***≡N), 121.44 (+, 2 Ph-***C***), 126.71 (+, 1 Ph-***C***), 126.79 (+, 1 Ph-***C***), 129.26 (+, 2 Ph-***C***), 128.62 (+, 2 Ph-***C***), 129.92 (+, 2 Ph-***C***), 134.60 (C$_{quat}$, 1 Ph-***C***), 150.98 (C$_{quat}$, 1 Ph-***C***), 163.88 (C$_{quat}$, ***C***═N). IR (cm^{-1}) = 3252 (N−H), 3212, 3065, 2190 (C≡N), 1635 (C═N), 1433, 1207. ES-MS (DCM/MeOH + NH_4OAc) *m*/*z* (%): 298 (100) [M + H]$^+$. Anal. ($C_{16}H_{15}N_3OS$) C, H, N. $C_{16}H_{15}N_3OS$ (297.37).

Compounds **27−31** and **33−43** were prepared by analogy (see Supporting Information).

Preparation of the Cyanoguanidines 48−78, 86, and 87. General Procedure. Hydrochlorides of **44** and **45** were converted into the bases by passing a basic ion exchanger (Merck, ion exchanger III, mobile phase MeOH). The respective isourea (1 equiv) and the pertinent amine (1.1 equiv) were refluxed in MeCN for 12 h. After removal of the solvent in vacuo, the crude product was purified by flash chromatography. For analytical purposes a small amount of most compounds was converted to the hydrogen oxalate by addition of a saturated solution of oxalic acid in Et_2O to a solution of the cyanoguanidine in EtOH.

2-Cyano-1-[4-(1*H*-imidazol-4-yl)butyl]-3-(2-phenylthioethyl)-guanidine (67). The title compound was prepared from **32** (0.60 g, 2.0 mmol) and **46** (0.31 g, 2.2 mmol) in MeCN (50 mL) according to the general procedure. The crude product was purified by flash chromatography ($CHCl_3$/MeOH/7 M NH_3 in MeOH, 92.5/5.5/2 v/v/v), yielding a colorless foamlike solid (0.42 g, 62%), mp (hydrogenoxalate) 130−133 °C. ^{1}H NMR (300 MHz, CD_3OD): δ [ppm] = 1.45−1.70 (m, 4H, Im-4-CH$_2$-C$\boldsymbol{H}_2$-C$\boldsymbol{H}_2$), 2.58 (t, 2H, ^3J = 7.1 Hz, Im-4-C$\boldsymbol{H}_2$), 3.07 (t, 2H, ^3J = 7.0 Hz, S-CH$_2$-C$\boldsymbol{H}_2$), 3.13 (t, 2H, ^3J = 6.9 Hz, Im-4-(CH$_2$)$_3$-C$\boldsymbol{H}_2$), 3.39 (t, 2H, ^3J = 7.0 Hz, S-C$\boldsymbol{H}_2$), 6.76 (d, 1H, ^4J = 1.1 Hz, 1H, Im-5-***H***), 7.10−7.41 (m, 5H, Ph-***H***), 7.53 (d, 1H, ^4J = 1.1 Hz, Im-2-***H***). ^{13}C NMR (75 MHz, CD_3OD): δ [ppm] = 27.17 (−, Im-4-***C***H$_2$), 27.67 (−, Im-4-CH$_2$-***C***H$_2$), 29.80 (−, Im-4-(CH$_2$)$_2$-***C***H$_2$), 33.53 (−, S-***C***H$_2$), 42.27 (−, Im-4-(CH$_2$)$_3$-***C***H$_2$), 42.61 (−, S-CH$_2$-***C***H$_2$), 117.88 (+, Im-***C***-5), 120.17 (C$_{quat}$, ***C***≡N), 127.30 (+, Ph-***C***-4), 130.16 (+, 2 Ph-***C***), 130.35 (+, 2 Ph-***C***), 135.76 (+, Im-***C***-2), 136.94 (C$_{quat}$, Ph-***C***-1), 138.10 (C$_{quat}$, Im-***C***-4), 161.02 (C$_{quat}$, ***C***═N). IR (cm^{-1}) = 3267 (N−H), 2989 (C−H), 2901 (C−H), 2159 (C≡N), 1576 (C═N). ES-MS (MeCN + TFA) *m*/*z* (%): 343 (100) [M + H]$^+$. HRMS (EI-MS) calcd for $C_{17}H_{22}N_6S$ [M$^{+\bullet}$] 342.1627; found 342.1625. Anal. ($C_{17}H_{22}N_6S \cdot 0.75C_2H_2O_4$) C, H, N. $C_{17}H_{22}N_6S$ (342.46).

Compounds **48−66**, **68−78**, **86**, and **87** were prepared by analogy (see Supporting Information).

Preparation of the Carbamoylguanidines 88−91. General Procedure. The pertinent cyanoguanidine was dissolved in 1 M HCl (25 mL) and left for 14 days at room temperature. After removing the solvent in vacuo, the crude product was purified by preparative HPLC, followed by flash chromatography under basic conditions to remove possible impurities with the corresponding guanidine.

2-Carbamoyl-1-[2-(1*H*-imidazol-4-yl)ethyl]-3-(3-phenylpropyl)-guanidine (88). The title compound was prepared from **48** (0.41 g, 1.38 mmol) according to the general procedure. Purification by preparative HPLC (MeCN/0.1% TFA (aq), 20/80) followed by flash chromatography ($CHCl_3$/MeOH/7 M NH_3 in MeOH, 90/8/2 v/v/v) yielded a colorless semisolid compound (0.35 g, 81%). ^{1}H NMR (300 MHz, CD_3OD, trifluoroacetate): δ [ppm] = 1.89−2.04 (m, 2H, Ph-CH$_2$-C$\boldsymbol{H}_2$), 2.70 (t, 2H, ^3J = 7.6 Hz, Ph-C$\boldsymbol{H}_2$), 3.07 (t, 2H, ^3J = 6.9 Hz, Im-4-C$\boldsymbol{H}_2$), 3.24−3.37 (m, 2H, overlap with solvent, Ph-CH$_2$-CH$_2$-C$\boldsymbol{H}_2$), 3.65 (t, 2H, ^3J = 6.9 Hz, Im-4-CH$_2$-C$\boldsymbol{H}_2$), 7.14−7.32 (m, 5H, Ph-***H***), 7.43 (d, 1H, ^4J = 1.2 Hz, Im-5-***H***), 8.84 (d, 1H, ^4J = 1.4 Hz, Im-2-***H***). ^{13}C NMR (75 MHz, CD_3OD, trifluoroacetate): δ [ppm] = 25.27 (−, Im-4-***C***H$_2$), 31.20 (−, Ph-CH$_2$-***C***H$_2$), 33.69 (−, Ph-***C***H$_2$), 41.37 (−, Im-4-***C***H$_2$), 42.45 (−, Ph-(CH$_2$)$_2$-***C***H$_2$), 118.19 (+, Im-***C***-5), 127.34 (+, Ph-***C***-4), 129.47 (+, 2 Ph-***C***), 129.67 (+, 2 Ph-***C***), 131.56 (C$_{quat}$, Im-***C***-4), 135.37 (+, Im-***C***-2), 142.07 (C$_{quat}$, Ph-***C***-1), 154.71 (C$_{quat}$, ***C***═N), 156.86 (C$_{quat}$, ***C***═O). IR (cm^{-1}) = 3153, 2930, 1662, 1603, 1181, 1128. ES-MS (H_2O/MeCN) *m*/*z* (%): 315 (100) [M + H]$^+$. HRMS (EI-MS) calcd for $C_{16}H_{22}N_6O$ [M$^{+\bullet}$] 314.1855; found 314.1860. $C_{16}H_{22}N_6O$ (314.39).

Compounds **89**, **90**, and **91** were prepared by analogy (see Supporting Information).

Preparation of the Trityl-Protected Sulfonylguanidines 92 and 93. 1-(4-Tosyl)-2-[3-(1-trityl-1*H*-imidazol-4-yl)propyl]guanidine (92). A mixture of **88**[31] (0.41 g, 1.0 mmol) and NaH (60% dispersion in mineral oil) (0.08 g, 2.0 mmol) in THF$_{abs}$ (15 mL) was stirred for 45 min at 50 °C. After the mixture was cooled to 0 °C, NEt_3 (0.28 mL, 2.0 mmol) and **90** (0.19 g, 1.0 mmol) in THF$_{abs}$ (15 mL) were subsequently added. Stirring was continued overnight at ambient temperature. After removal of the solvent in vacuo, the crude product was purified by flash chromatography ($CHCl_3$/MeOH/NH_3 (aq) 32%, 80/9/1 v/v/v), yielding a colorless foamlike solid (0.22 g, 39%). ^{1}H NMR (300 MHz, $CDCl_3$): δ [ppm] = 1.73−1.94 (m, 2H, Im-4-CH$_2$-C$\boldsymbol{H}_2$), 2.36 (s, 3H, C$\boldsymbol{H}_3$),

2.44−2.79 (m, 2H, Im-4-CH_2), 3.25−3.42 (m, 2H, Im-4-$(CH_2)_2$-CH_2), 6.72 (s, 1H, Im-5-***H***), 7.06−7.15 (m, 6H, Ph-***H***), 7.19 (d, 2H, ^3J = 8.0 Hz, Ph-3,5-***H***), 7.30−7.45 (m, 10H, Ph-***H*** + Im-2-***H***), 7.74 (d, 2H, ^3J = 8.0 Hz, Ph-2,6-***H***). ES-MS (DCM/MeOH + NH_4OAc) *m*/*z* (%): 564 (100) $[M + H]^+$. $C_{33}H_{33}N_5O_2S$ (563.71).

1-(*tert*-Butoxycarbonyl)-2-(2-phenylethylsulfonyl)-1-[3-(1-trityl-1*H*-imidazol-4-yl)propyl]guanidine (93). To a solution of **89**[34] (0.51 g, 1.0 mmol) and DIEA (0.39 g, 3.0 mmol) in DCM (20 mL), **91**[65] (0.21 g, 1.0 mmol) dissolved in DCM (10 mL) was added dropwise at 0 °C. After 1 h, stirring was continued overnight at room temperature and the solvent was evaporated. The crude product was purified by flash chromatography ($CHCl_3$/MeOH, 97.5/2.5 v/v), yielding the title compound as colorless oil (0.34 g, 50%). ^{1}H NMR (300 MHz, $CDCl_3$) isomers: δ [ppm] = 1.47 (s, 3H, C(CH_3)$_3$), 1.49 (s, 6H, C(CH_3)$_3$), 1.86−1.91 (m, 2H, Im-4-CH_2-CH_2), 2.51−2.63 (m, 2H, Im-4-CH_2), 3.04−3.17 (m, 2H, Ph-CH_2), 3.23−3.35 (m, 2H, Ph-CH_2-CH_2), 3.76−3.85 (m, 2H, Im-4-$(CH_2)_2$-CH_2), 6.53 (d, 0.7H, ^4J = 1.3 Hz, Im-5-***H***), 6.55 (d, 0.3H, ^4J = 1.3 Hz, Im-5-***H***), 7.06−7.38 (m, 21H, Ph-***H*** + Im-2-***H***). ES-MS (DCM/MeOH + NH_4OAc) *m*/*z* (%): 678 (100) $[M + H]^+$. $C_{39}H_{43}N_5O_4S$ (677.85).

Preparation of the Sulfonylguanidines 94 and 95. 1-[3-(1*H*-Imidazol-4-yl)propyl]-2-(4-tosyl)guanidine (94). A mixture of **92** (0.19 g, 0.34 mmol) and TFA (5 mL) in DCM (20 mL) was stirred for 5 h. After evaporation of the solvent, the crude product was purified by preparative HPLC (MeCN/0.1% TFA (aq), 25/75), yielding the title compound as a colorless semisolid (0.12 g, 82%). ^{1}H NMR (300 MHz, CD_3OD, trifluoroacetate): δ [ppm] = 1.76−1.92 (m, 2H, Im-4-CH_2-CH_2), 2.38 (s, 3H, CH_3), 2.70 (t, 2H, ^3J = 7.3 Hz, Im-4-CH_2), 3.23 (t, 2H, ^3J = 6.7 Hz, Im-4-$(CH_2)_2$-CH_2), 7.29 (d, 2H, ^3J = 8.3 Hz, Ph-3-***H***), 7.33 (s, 1H, Im-5-***H***), 7.72 (d, 2H, ^3J = 8.3 Hz, Ph-2-***H***), 8.76 (d, 1H, ^4J = 1.4 Hz, Im-2-***H***). ^{13}C NMR (75 MHz, CD_3OD, trifluoroacetate): δ [ppm] = 21.46 (+, ***C***H$_3$), 22.35 (−, Im-4-***C***H$_2$), 29.64 (−, Im-4-CH_2-***C***H$_2$), 40.67 (−, Im-4-$(CH_2)_2$-***C***H$_2$), 117.02 (+, Im-***C***-5), 127.21 (+, 2 Ph-***C***-2), 130.41 (+, 2 Ph-***C***-3), 134.67 (+, Im-***C***-2), 134.85 (C_{quat}, Im-***C***-4), 141.99 (C_{quat}, Ph-***C***-1), 143.83 (C_{quat}, Ph-***C***-4), 158.70 (C_{quat}, ***C***=N). IR (cm^{-1}) = 3159, 2989, 2901, 1663, 1624, 1548, 1166, 1128, 1081. HRMS (EI-MS) calcd for $C_{14}H_{19}N_5O_2S$ [$M^{+\bullet}$] 321.1259; found 321.1257. $C_{14}H_{19}N_5O_2S \cdot$TFA (435.42).

1-[3-(1*H*-Imidazol-4-yl)propyl]-2-(2-phenylethylsulfonyl)guanidine (95). A mixture of **93** (0.30 g, 0.44 mmol) and TFA (5 mL) in DCM (20 mL) was stirred for 5 h. After evaporation of the solvent, the crude product was purified by preparative HPLC (MeCN/0.1% TFA (aq), 25/75), yielding the title compound as colorless semisolid (0.14 g, 71%). ^{1}H NMR (300 MHz, CD_3OD, trifluoroacetate): δ [ppm] = 1.82−1.96 (m, 2H, Im-4-CH_2-CH_2), 2.76 (t, 2H, ^3J = 7.3 Hz, Im-4-CH_2), 3.01−3.11 (m, 2H, Ph-CH_2), 3.19 (t, 2H, ^3J = 6.9 Hz, Im-4-$(CH_2)_2$-CH_2), 3.23−3.29 (m, 2H, Ph-CH_2-CH_2), 7.15−7.31 (m, 5H, Ph-***H***), 7.37 (s, 1H, ^4J = 1.3 Hz, Im-5-***H***), 8.76 (d, 1H, ^4J = 1.3 Hz, Im-2-***H***). ^{13}C NMR (75 MHz, CD_3OD, trifluoroacetate): δ [ppm] = 22.42 (−, Im-4-***C***H$_2$), 29.48 (−, Im-4-CH_2-***C***H$_2$), 31.42 (−, Ph-***C***H$_2$), 40.63 (−, Im-4-$(CH_2)_2$-***C***H$_2$), 56.24 (−, Ph-CH_2-***C***H$_2$), 117.07 (+, Im-***C***-5), 127.66 (+, Ph-***C***-4), 129.44 (+, 2 Ph-***C***), 129.77 (+, 2 Ph-***C***), 134.70 (+, Im-***C***-2), 134.89 (C_{quat}, Im-***C***-4), 140.27 (C_{quat}, Ph-***C***-1), 158.95 (C_{quat}, ***C***=N). IR (cm^{-1}) = 3149, 2972, 2901, 1666, 1625, 1554, 1186, 1131, 1101. HRMS (EI-MS) calcd for $C_{15}H_{21}N_5O_2S$ [$M^{+\bullet}$] 335.1416; found 335.1421. $C_{15}H_{21}N_5O_2S \cdot$TFA (449.45).

Pharmacological Methods. Materials. Histamine dihydrochloride was purchased from Alfa Aesar GmbH & Co. KG (Karlsruhe, Germany). Thioperamide maleate and iodophenpropit dihydrobromide were from Tocris Bioscience (Ellisville, MO). The H_4R antagonist **1** was synthesized according to ref 23. [^{3}H]-Mepyramine, [^{3}H]tiotidine, [^{3}H]*N*$^\alpha$-methylhistamine, and [^{3}H]-histamine were from PerkinElmer Life Sciences (Boston, MA). [γ-^{32}P]GTP was synthesized according to a previously described method.[66] [^{32}P]P_i (8500−9100 Ci/mmol orthophosphoric acid) was from PerkinElmer Life Sciences (Boston, MA). All unlabeled nucleotides, glycerol 3-phosphate dehydrogenase, triose phosphate isomerase, glyceraldehyde 3-phosphate dehydrogenase, and lactate dehydrogenase were from Roche (Mannheim, Germany). 3-Phosphoglycerate kinase and L-α-glycerol phosphate were from Sigma. GF/C filters were from Whatman (Maidstone, U.K.).

Data Analysis and Pharmacological Parameters. All data are presented as the mean of *n* independent experiments ± SEM. Agonist potencies were given as pEC_{50} values (negative decadic logarithm of the molar concentration of the agonist causing 50% of the maximal response). Maximal responses (intrinsic activities) were expressed as α values. The α value of histamine was set to 1.00, and α values of other compounds were referenced to this value.

IC_{50} values were converted to K_I and K_B values using the Cheng−Prussoff equation.[67] pK_I values were analyzed by nonlinear regression and best-fit to one-site (monophasic) competition isotherms. pEC_{50} and pK_B values from the functional GTPase assays were analyzed by nonlinear regression and best-fit to sigmoidal dose−response curves (GraphPad Prism, version 4.02 software, San Diego, CA).

Steady-State GTPase Activity Assay. GTPase activity assays were performed as previously described.[31,43,44,68] For H_1R assays, Sf9 insect cell membranes coexpressing the hH_1R and RGS4 were employed. For H_2R assays, Sf9 insect cell membranes expressing the hH_2R-$G_{s\alpha S}$ fusion protein were used. For H_3R assays, Sf9 insect cell membranes coexpressing the hH_3R, mammalian $G_{i\alpha 2}$, $G_{\beta 1\gamma 2}$, and RGS4 were employed. For H_4R assays, Sf9 insect cell membranes coexpressing the hH_4R-RGS19 fusion protein and mammalian $G_{i\alpha 2}$ and $G_{\beta 1\gamma 2}$ were used. The respective membranes were thawed and sedimented by centrifugation at 4 °C and 13000*g* for 10 min. Membranes were resuspended in 10 mM Tris-HCl, pH 7.4. Each assay tube contained Sf9 membranes expressing the respective HR subtype (10−20 μg protein/tube), $MgCl_2$ ($H_{1,2}R$ assays, 1.0 mM; $H_{3,4}R$ assays, 5.0 mM), 100 μM EDTA, 100 μM ATP, 100 nM GTP, 100 μM adenylyl imidophosphate, 5 mM creatine phosphate, 40 μg of creatine kinase, and 0.2% (w/v) bovine serum albumin in 50 mM Tris/HCl, pH 7.4, and the investigated ligands at various concentrations. All H_4R assays additionally contained 100 mM NaCl. For the determination of pK_B values (antagonist mode of the GTPase activity assay) histamine was added to the reaction mixtures (final concentrations: H_1R, 200 nM; H_2R, 1 μM; $H_{3,4}R$, 100 nM).

Reaction mixtures (80 μL) were incubated for 2 min at 25 °C. After the addition of 20 μL of [γ-^{32}P]GTP (0.1 μCi/tube), reaction mixtures were incubated for 20 min at 25 °C. Reactions were terminated by the addition of 900 μL of slurry consisting of 5% (w/v) activated charcoal and 50 mM NaH_2PO_4, pH 2.0. Charcoal absorbs nucleotides but not P_i. Charcoal-quenched reaction mixtures were centrifuged for 7 min at room temperature at 13000*g*. An amount of 600 μL of the supernatant was removed, and $^{32}P_i$ was determined by liquid scintillation counting. Spontaneous [γ-^{32}P]GTP degradation was determined in tubes containing all components described above, plus a high concentration of unlabeled GTP (1 mM) that due to competition with [γ-^{32}P]GTP prevents [γ-^{32}P]GTP hydrolysis by enzymatic activities present in Sf9 membranes. Spontaneous [γ-^{32}P]GTP degradation was <1% of the total amount of radioactivity added. The experimental conditions chosen ensured that not more than 10% of the total amount of [γ-^{32}P]GTP added was converted to $^{32}P_i$.

Radioligand Binding Assays. For the binding experiments, the Sf9 insect cell membranes described above were employed. The respective membranes were thawed and sedimented by centrifugation at 4 °C and 13000*g* for 10 min. Membranes were resuspended in binding buffer (12.5 mM $MgCl_2$, 1 mM EDTA, and 75 mM Tris/HCl, pH 7.4). Each tube (total volume 500 μL) contained 50 μg (hH_1R, hH_3R), 120 μg (hH_4R), or 250 μg (hH_2R) of membrane protein. Competition binding experiments

were performed in the presence of 5 nM [^{3}H]mepyramine (hH_1R), 10 nM [^{3}H]tiotidine (hH_2R), 3 nM [^{3}H]N^{α}-methylhistamine (hH_3R), or 10 nM [^{3}H]histamine (hH_4R) and increasing concentrations of unlabeled ligands. Incubations were conducted for 60 min at 25 °C and shaking at 250 rpm. Bound radioligand was separated from free radioligand by filtration through 0.3% polyethyleneimine-pretreated GF/C filters, followed by three washes with 2 mL of cold binding buffer (4 °C) using a Brandel harvester. Filter-bound radioactivity was determined after an equilibration phase of at least 12 h by liquid scintillation counting.

Molecular Modeling. First, a rough model of the hH_4R was directly constructed from the PDB file 2RH1 of the β_2-adrenoceptor crystal structure,[49] using the software suite SYBYL 7.3 (Tripos, L.P., St. Louis, MO) on a SGI Octane workstation. The backbone coordinates of TMs 1−7, helix 8, the C1 loop, and identical side chains were retained. All other cocrystallized substructures and the lysozyme domain were deleted. The C3 loop was truncated; only the first two and the last five positions were transferred, and the gap was closed by five alanine residues. All other loop regions were constructed by Sybyl loop searches. The side chains differing between the β_2-adrenoceptor and the hH_4R were mutated.

The resulting model was prepared for optimization by adding hydrogens and providing atoms with Amber-FF99 charges.[69] Bad contacts of side chains were removed using the Lovell rotamer library.[70] Subsequently, the model was roughly minimized (25 cycles of steepest descent with fixed TM backbone, 100 cycles of Powell conjugated gradient, Amber-FF99 force field,[69] distant dependent dielectric constant $\varepsilon = 4$) and checked for inconsistencies of the local geometry with Sybyl ProTable. To test the influence of alternative side chain rotamer conformations, molecular dynamics (MD) simulations were performed following a protocol published in detail elsewhere.[71] In brief, the model was embedded into an environment consisting of 93 1-palmitoyl-2-oleoylphosphatidylcholine molecules, 14 429 intracellular and extracellular water molecules, and 8 Na^+ and 24 Cl^- ions to achieve electroneutrality, and the whole complex was energetically minimized. The 1.35 ns equilibrium phase of the MD was divided into one 250 ps and eleven 100 ps cycles with gradually descending constraints for the backbone and the side chain atoms. Then, a 1 ns productive phase without constraints was performed. The simulations were carried out at 310 K and 1 atm with Berendsen, temperature, and pressure coupling using the software package GROMACS 3.2[72] with the ffG53A6 force field.[73]

The final snapshot of the MD simulation was roughly minimized (SYBYL 7.3, Amber-FF99 force field). Compound **67** was manually docked into the model in an energetically favorable conformation, considering results of previous in vitro mutagenesis[51] and theoretical studies.[52] Then the same MD simulation protocol as described above was applied to the ligand−hH_4R complex. Parameters for compound **67** were adopted from the ffG53A6 force field. The ligand−hH_4R complex from the final (1 ns) snapshot of the productive phase was extracted and gradually minimized using SYBYL 7.3: (1) ligand fixed and provided with Gasteiger−Huckel charges, Amber-FF99 force field, distant dependent $\varepsilon = 4$, 25 cycles of steepest descent, then Powell algorithm; (2) compound **67** and a region of 6 Å around, Tripos force field,[74] distant dependent $\varepsilon = 1$, Powell method, and rms gradient of 0.05 kcal mol^{-1}; (3) as in step 1, Powell method, and rms gradient 0.01 kcal mol^{-1}. The rms deviation of the TM backbones between the resulting model and the β_2-adrenoceptor crystal structure 2RH1 amounts to 1.07 Å.

Acknowledgment. The authors are grateful to Kerstin Fisch, Karin Schadendorf, Gertraud Wilberg, and Astrid Seefeld for expert technical assistance, to Dr. Erich Schneider for helpful discussions, to Dr. Robin Thurmond (Department of Immunology, Johnson & Johnson Pharmaceutical R&D, San Diego, CA) for hH_3R cDNA, and to David Schnell for providing the hH_3R baculovirus. This work was supported by the Graduate Training Program (Graduiertenkolleg) GRK 760, "Medicinal Chemistry: Molecular Recognition, Ligand−Receptor Interactions", of the Deutsche Forschungsgemeinschaft and the COST program BM0806 (H_4R network) of the European Union.

Supporting Information Available: Synthetic procedures and analytical data for compounds **27**−**31**, **33**−**43**, **45**, **46**, **48**−**66**, **68**−**84**, **86**, **87**, and **89**−**91**; purity data (elemental analysis results, HPLC data) of all target compounds. This material is available free of charge via the Internet at http://pubs.acs.org.

References

(1) Hill, S. J.; Ganellin, C. R.; Timmerman, H.; Schwartz, J.-C.; Shankley, N. P.; Young, J. M.; Schunack, W.; Levi, R.; Haas, H. L. International Union of Pharmacology. XIII. Classification of histamine receptors. *Pharmacol. Rev.* **1997**, *49*, 253–278.
(2) Hough, L. B. Genomics meets histamine receptors: new subtypes, new receptors. *Mol. Pharmacol.* **2001**, *59*, 415–419.
(3) Schlicker, E.; Kathmann, M. Modulation of in vitro neurotransmission in the CNS and in the retina via H_3 heteroreceptors. *Pharmacochem. Libr.* **1998**, *30*, 13–26.
(4) Sander, K.; Kottke, T.; Stark, H. Histamine h(3) receptor antagonists go to clinics. *Biol. Pharm. Bull.* **2008**, *31*, 2163–2181.
(5) Oda, T.; Morikawa, N.; Saito, Y.; Masuho, Y.; Matsumoto, S. Molecular cloning and characterization of a novel type of histamine receptor preferentially expressed in leukocytes. *J. Biol. Chem.* **2000**, *275*, 36781–36786.
(6) Nakamura, T.; Itadani, H.; Hidaka, Y.; Ohta, M.; Tanaka, K. Molecular cloning and characterization of a new human histamine receptor, hH_4R. *Biochem. Biophys. Res. Commun.* **2000**, *279*, 615–620.
(7) Zhu, Y.; Michalovich, D.; Wu, H.-L.; Tan, K. B.; Dytko, G. M.; Mannan, I. J.; Boyce, R.; Alston, J.; Tierney, L. A.; Li, X.; Herrity, N. C.; Vawter, L.; Sarau, H. M.; Ames, R. S.; Davenport, C. M.; Hieble, J. P.; Wilson, S.; Bergsma, D. J.; Fitzgerald, L. R. Cloning, expression, and pharmacological characterization of a novel human histamine receptor. *Mol. Pharmacol.* **2001**, *59*, 434–441.
(8) Morse, K. L.; Behan, J.; Laz, T. M.; West, R. E., Jr.; Greenfeder, S. A.; Anthes, J. C.; Umland, S.; Wan, Y.; Hipkin, R. W.; Gonsiorek, W.; Shin, N.; Gustafson, E. L.; Qiao, X.; Wang, S.; Hedrick, J. A.; Greene, J.; Bayne, M.; Monsma, F. J., Jr. Cloning and characterization of a novel human histamine receptor. *J. Pharmacol. Exp. Ther.* **2001**, *296*, 1058–1066.
(9) O'Reilly, M.; Alpert, R.; Jenkinson, S.; Gladue, R. P.; Foo, S.; Trim, S.; Peter, B.; Trevethick, M.; Fidock, M. Identification of a histamine H_4 receptor on human eosinophils. Role in eosinophil chemotaxis. *J. Recept. Signal Transduction Res.* **2002**, *22*, 431–448.
(10) Coge, F.; Guenin, S.-P.; Rique, H.; Boutin, J. A.; Galizzi, J.-P. Structure and expression of the human histamine H_4-receptor gene. *Biochem. Biophys. Res. Commun.* **2001**, *284*, 301–309.
(11) Nguyen, T.; Shapiro, D. A.; George, S. R.; Setola, V.; Lee, D. K.; Cheng, R.; Rauser, L.; Lee, S. P.; Lynch, K. R.; Roth, B. L.; O'Dowd, B. F. Discovery of a novel member of the histamine receptor family. *Mol. Pharmacol.* **2001**, *59*, 427–433.
(12) Liu, C.; Ma, X.-J.; Jiang, X.; Wilson, S. J.; Hofstra, C. L.; Blevitt, J.; Pyati, J.; Li, X.; Chai, W.; Carruthers, N.; Lovenberg, T. W. Cloning and pharmacological characterization of a fourth histamine receptor (H_4) expressed in bone marrow. *Mol. Pharmacol.* **2001**, *59*, 420–426.
(13) Gantner, F.; Sakai, K.; Tusche, M. W.; Cruikshank, W. W.; Center, D. M.; Bacon, K. B. Histamine H_4 and H_2 receptors control histamine-induced interleukin-16 release from human $CD8^+$ T cells. *J. Pharmacol. Exp. Ther.* **2002**, *303*, 300–307.
(14) Hofstra, C. L.; Desai, P. J.; Thurmond, R. L.; Fung-Leung, W.-P. Histamine H_4 receptor mediates chemotaxis and calcium mobilization of mast cells. *J. Pharmacol. Exp. Ther.* **2003**, *305*, 1212–1221.
(15) Lippert, U.; Artuc, M.; Grutzkau, A.; Babina, M.; Guhl, S.; Haase, I.; Blaschke, V.; Zachmann, K.; Knosalla, M.; Middel, P.; Kruger-Krasagakis, S.; Henz, B. M. Human skin mast cells express H_2 and H_4, but not H_3 receptors. *J. Invest. Dermatol.* **2003**, *123*, 116–123.
(16) Buckland, K. F.; Williams, T. J.; Conroy, D. M. Histamine induces cytoskeletal changes in human eosinophils via the H_4 receptor. *Br. J. Pharmacol.* **2003**, *140*, 1117–1127.
(17) Takeshita, K.; Sakai, K.; Bacon, K. B.; Gantner, F. Critical role of histamine H_4 receptor in leukotriene B_4 production and mast

cell-dependent neutrophil recruitment induced by zymosan in vivo. *J. Pharmacol. Exp. Ther.* **2003**, *307*, 1072–1078.
(18) Dijkstra, D.; Leurs, R.; Chazot, P.; Shenton, F. C.; Stark, H.; Werfel, T.; Gutzmer, R. Histamine downregulates monocyte CCL2 production through the histamine H_4 receptor. *J. Allergy Clin. Immunol.* **2007**, *120*, 300–307.
(19) Thurmond, R. L.; Desai, P. J.; Dunford, P. J.; Fung-Leung, W.-P.; Hofstra, C. L.; Jiang, W.; Nguyen, S.; Riley, J. P.; Sun, S.; Williams, K. N.; Edwards, J. P.; Karlsson, L. A potent and selective histamine H_4 receptor antagonist with anti-inflammatory properties. *J. Pharmacol. Exp. Ther.* **2004**, *309*, 404–413.
(20) Coruzzi, G.; Adami, M.; Guaita, E.; de Esch, I. J. P.; Leurs, R. Antiinflammatory and antinociceptive effects of the selective histamine H_4-receptor antagonists JNJ7777120 and VUF6002 in a rat model of carrageenan-induced acute inflammation. *Eur. J. Pharmacol.* **2007**, *563*, 240–244.
(21) Smits, R. A.; Lim, H. D.; Hanzer, A.; Zuiderveld, O. P.; Guaita, E.; Adami, M.; Coruzzi, G.; Leurs, R.; de Esch, I. J. P. Fragment based design of new H_4 receptor-ligands with anti-inflammatory properties in vivo. *J. Med. Chem.* **2008**, *51*, 2457–2467.
(22) Dunford, P. J.; O'Donnell, N.; Riley, J. P.; Williams, K. N.; Karlsson, L.; Thurmond, R. L. The histamine H_4 receptor mediates allergic airway inflammation by regulating the activation of $CD4^+$ T cells. *J. Immunol.* **2006**, *176*, 7062–7070.
(23) Jablonowski, J. A.; Grice, C. A.; Chai, W.; Dvorak, C. A.; Venable, J. D.; Kwok, A. K.; Ly, K. S.; Wei, J.; Baker, S. M.; Desai, P. J.; Jiang, W.; Wilson, S. J.; Thurmond, R. L.; Karlsson, L.; Edwards, J. P.; Lovenberg, T. W.; Carruthers, N. I. The first potent and selective non-imidazole human histamine H_4 receptor antagonists. *J. Med. Chem.* **2003**, *46*, 3957–3960.
(24) Dunford, P. J.; Williams, K. N.; Desai, P. J.; Karlsson, L.; McQueen, D.; Thurmond, R. L. Histamine H_4 receptor antagonists are superior to traditional antihistamines in the attenuation of experimental pruritus. *J. Allergy Clin. Immunol.* **2007**, *119*, 176–183.
(25) Jablonowski, J. A.; Carruthers, N. I.; Thurmond, R. L. The histamine H_4 receptor and potential therapeutic uses for H_4 ligands. *Mini-Rev. Med. Chem.* **2004**, *4*, 993–1000.
(26) Lim, H. D.; van Rijn, R. M.; Ling, P.; Bakker, R. A.; Thurmond, R. L.; Leurs, R. Evaluation of histamine H_1-, H_2-, and H_3-receptor ligands at the human histamine H_4 receptor: identification of 4-methylhistamine as the first potent and selective H_4 receptor agonist. *J. Pharmacol. Exp. Ther.* **2005**, *314*, 1310–1321.
(27) Arrang, J. M.; Garbarg, M.; Lancelot, J. C.; Lecomte, J. M.; Pollard, H.; Robba, M.; Schunack, W.; Schwartz, J. C. Highly potent and selective ligands for histamine H3-receptors. *Nature* **1987**, *327*, 117–123.
(28) Morisset, S.; Rouleau, A.; Ligneau, X.; Gbahou, F.; Tardivel-Lacombe, J.; Stark, H.; Schunack, W.; Ganellin, C. R.; Schwartz, J. C.; Arrang, J. M. High constitutive activity of native H3 receptors regulates histamine neurons in brain. *Nature* **2000**, *408*, 860–864.
(29) Lim, H. D.; Smits, R. A.; Bakker, R. A.; van Dam, C. M. E.; de Esch, I. J. P.; Leurs, R. Discovery of *S*-(2-guanidylethyl)-isothiourea (VUF 8430) as a potent nonimidazole histamine H_4 receptor agonist. *J. Med. Chem.* **2006**, *49*, 6650–6651.
(30) Hashimoto, T.; Harusawa, S.; Araki, L.; Zuiderveld, O. P.; Smit, M. J.; Imazu, T.; Takashima, S.; Yamamoto, Y.; Sakamoto, Y.; Kurihara, T.; Leurs, R.; Bakker, R. A.; Yamatodani, A. A selective human H_4-receptor agonist: (−)-2-cyano-1-methyl-3-{(2*R*,5*R*)-5-[1*H*-imidazol-4(5)-yl]tetrahydrofuran-2-yl}methylguanidine. *J. Med. Chem.* **2003**, *46*, 3162–3165.
(31) Ghorai, P.; Kraus, A.; Keller, M.; Gotte, C.; Igel, P.; Schneider, E.; Schnell, D.; Bernhardt, G.; Dove, S.; Zabel, M.; Elz, S.; Seifert, R.; Buschauer, A. Acylguanidines as bioisosteres of guanidines: N^G-acylated imidazolylpropylguanidines, a new class of histamine H_2 receptor agonists. *J. Med. Chem.* **2008**, *51*, 7193–7204.
(32) Xie, S.-X.; Kraus, A.; Ghorai, P.; Ye, Q.-Z.; Elz, S.; Buschauer, A.; Seifert, R. N^1-(3-Cyclohexylbutanoyl)-N^2-[3-(1*H*-imidazol-4-yl)-propyl]guanidine (UR-AK57), a potent partial agonist for the human histamine H_1- and H_2-receptors. *J. Pharmacol. Exp. Ther.* **2006**, *317*, 1262–1268.
(33) Xie, S.-X.; Ghorai, P.; Ye, Q.-Z.; Buschauer, A.; Seifert, R. Probing ligand-specific histamine H_1- and H_2-receptor conformations with N^G-acylated imidazolylpropylguanidines. *J. Pharmacol. Exp. Ther.* **2006**, *317*, 139–146.
(34) Igel, P.; Schneider, E.; Schnell, D.; Elz, S.; Seifert, R.; Buschauer, A. N^G-Acylated imidazolylpropylguanidines as potent histamine H_4 receptor agonists: selectivity by variation of the N^G-substituent. *J. Med. Chem.* **2009**, *52*, 2623–2627.
(35) Igel, P.; Schnell, D.; Bernhardt, G.; Seifert, R.; Buschauer, A. Tritium-labeled *N*(1)-[3-(1*H*-imidazol-4-yl)propyl]-*N*(2)-propionylguanidine ([(3)H]UR-PI294), a high-affinity histamine H(3) and H(4) receptor radioligand. *ChemMedChem* **2009**, *4*, 225–231.
(36) pK_a value was calculated with the following: *ACD Labs 9.0*; Advanced Chemistry Development: Toronto, Canada.
(37) Durant, G. J.; Emmett, J. C.; Ganellin, C. R.; Miles, P. D.; Parsons, M. E.; Prain, H. D.; White, G. R. Cyanoguanidine−thiourea equivalence in the development of the histamine H_2-receptor antagonist, cimetidine. *J. Med. Chem.* **1977**, *20*, 901–906.
(38) Durant, G. J.; Ganellin, C. R.; Hills, D. W.; Miles, P. D.; Parsons, M. E.; Pepper, E. S.; White, G. R. The histamine H_2 receptor agonist impromidine: synthesis and structure−activity considerations. *J. Med. Chem.* **1985**, *28*, 1414–1422.
(39) Kraus, A. Highly Potent, Selective Acylguanidine-Type Histamine H2 Receptor Agonists: Synthesis and Structure−Activity Relationships. Ph.D. Thesis, University of Regensburg, Regensburg, Germany, **2007**; http://www.opus-bayern.de/uni-regensburg/frontdoor.php?source_opus=904&la=de.
(40) Buschauer, A. Synthesis and pharmacological activity of arylmethylthioethylguanidines. *Arzneim.-Forsch.* **1987**, *37* (II), 1008–1012.
(41) Webb, R. L.; Eggleston, D. S.; Labaw, C. S.; Lewis, J. J.; Wert, K. Diphenyl cyancarbonimidate and dichlorodiphenoxymethane as synthons for the construction of heterocyclic systems of medicinal interest. *J. Heterocycl. Chem.* **1987**, *24*, 275–278.
(42) Webb, R. L.; Labaw, C. S. Diphenyl cyanocarbonimidate. a versatile synthon for the construction of heterocyclic systems. *J. Heterocycl. Chem.* **1982**, *19*, 1205–1206.
(43) Kelley, M. T.; Burckstummer, T.; Wenzel-Seifert, K.; Dove, S.; Buschauer, A.; Seifert, R. Distinct interaction of human and guinea pig histamine H_2-receptor with guanidine-type agonists. *Mol. Pharmacol.* **2001**, *60*, 1210–1225.
(44) Seifert, R.; Wenzel-Seifert, K.; Burckstummer, T.; Pertz, H. H.; Schunack, W.; Dove, S.; Buschauer, A.; Elz, S. Multiple differences in agonist and antagonist pharmacology between human and guinea pig histamine H_1-receptor. *J. Pharmacol. Exp. Ther.* **2003**, *305*, 1104–1115.
(45) Lim, H. D.; Jongejan, A.; Bakker, R. A.; Haaksma, E.; de Esch, I. J. P.; Leurs, R. Phenylalanine 169 in the second extracellular loop of the human histamine H-4 receptor is responsible for the difference in agonist binding between human and mouse H-4 receptors. *J. Pharmacol. Exp. Ther.* **2008**, *327*, 88–96.
(46) Altenbach, R. J.; Adair, R. M.; Bettencourt, B. M.; Black, L. A.; Fix-Stenzel, S. R.; Gopalakrishnan, S. M.; Hsieh, G. C.; Liu, H.; Marsh, K. C.; McPherson, M. J.; Milicic, I.; Miller, T. R.; Vortherms, T. A.; Warrior, U.; Wetter, J. M.; Wishart, N.; Witte, D. G.; Honore, P.; Esbenshade, T. A.; Hancock, A. A.; Brioni, J. D.; Cowart, M. D. Structure−activity studies on a series of a 2-aminopyrimidine-containing histamine H4 receptor ligands. *J. Med. Chem.* **2008**, *51*, 6571–6580.
(47) Schnell, D. Department of Pharmacology and Toxicology, University of Regensburg, Germany. Personal communication, 2009.
(48) Jansen, F. P.; Rademaker, B.; Bast, A.; Timmerman, H. The first radiolabeled histamine H3 receptor antagonist, [^{125}I]iodophenpropit: saturable and reversible binding to rat cortex membranes. *Eur. J. Pharmacol.* **1992**, *217*, 203–205.
(49) Cherezov, V.; Rosenbaum, D. M.; Hanson, M. A.; Rasmussen, S. G.; Thian, F. S.; Kobilka, T. S.; Choi, H. J.; Kuhn, P.; Weis, W. I.; Kobilka, B. K.; Stevens, R. C. High-resolution crystal structure of an engineered human beta2-adrenergic G protein-coupled receptor. *Science* **2007**, *318*, 1258–1265.
(50) Rosenbaum, D. M.; Cherezov, V.; Hanson, M. A.; Rasmussen, S. G.; Thian, F. S.; Kobilka, T. S.; Choi, H. J.; Yao, X. J.; Weis, W. I.; Stevens, R. C.; Kobilka, B. K. GPCR engineering yields high-resolution structural insights into beta2-adrenergic receptor function. *Science* **2007**, *318*, 1266–1273.
(51) Shin, N.; Coates, E.; Murgolo, N. J.; Morse, K. L.; Bayne, M.; Strader, C. D.; Monsma, F. J., Jr. Molecular modeling and site-specific mutagenesis of the histamine-binding site of the histamine H4 receptor. *Mol. Pharmacol.* **2002**, *62*, 38–47.
(52) Jongejan, A.; Lim, H. D.; Smits, R. A.; de Esch, I. J. P.; Haaksma, E.; Leurs, R. Delineation of agonist binding to the human histamine H-4 receptor using mutational analysis, homology modeling, and ab initio calculations. *J. Chem. Inf. Model.* **2008**, *48*, 1455–1463.
(53) Arbuznikov, A. V.; Sheludyakova, L. A.; Burgina, E. B. Ab-initio study of cyanoguanidine isomers. *Chem. Phys. Lett.* **1995**, *240*, 239–244.
(54) Bach, R. D.; Mcdouall, J. J. W.; Owensby, A. L.; Schlegel, H. B.; Holubka, J. W.; Ball, J. C. Structure and dynamics of dicyandiamide: a theoretical study. *J. Phys. Org. Chem.* **1991**, *4*, 125–134.
(55) Ballesteros, J. A.; Weinstein, H. Integrated methods for the construction of three-dimensional models and computational probing

of structure−function relations in G protein-coupled receptors. *Methods Neurosci.* **1995**, *25*, 366–428.
(56) Prout, K.; Critchle, Sr.; Ganellin, C. R. 2-(4-Imidazolyl)ethylammonium bromide (histamine monohydrobromide). *Acta Crystallogr. B* **1974**, *30*, 2884–2886.
(57) Preuss, H.; Ghorai, P.; Kraus, A.; Dove, S.; Buschauer, A.; Seifert, R. Mutations of Cys-17 and Ala-271 in the human histamine H2 receptor determine the species selectivity of guanidine-type agonists and increase constitutive activity. *J. Pharmacol. Exp. Ther.* **2007**, *321*, 975–982.
(58) Lei, S.; Liapakis, G.; Xu, R.; Guarnieri, F.; Ballesteros, J. A.; Javitch, J. A. Beta(2) adrenergic receptor activation. Modulation of the proline kink in transmembrane 6 by a rotamer toggle switch. *J. Biol. Chem.* **2002**, *277*, 40989–40996.
(59) Seifert, R.; Wenzel-Seifert, K.; Kobilka, B. K. GPCR-Galpha fusion proteins: molecular analysis of receptor-G-protein coupling. *Trends Pharmacol. Sci.* **1999**, *20*, 383–389.
(60) Klinker, J. F.; Hageluken, A.; Grunbaum, L.; Heilmann, I.; Nurnberg, B.; Harhammer, R.; Offermanns, S.; Schwaner, I.; Ervens, J.; Wenzel-Seifert, K. Mastoparan may activate GTP hydrolysis by Gi-proteins in HL-60 membranes indirectly through interaction with nucleoside diphosphate kinase. *Biochem. J.* **1994**, *304* (Part 2), 377–383.
(61) Hageluken, A.; Grunbaum, L.; Klinker, J. F.; Nurnberg, B.; Harhammer, R.; Schultz, G.; Leschke, C.; Schunack, W.; Seifert, R. Histamine receptor-dependent and/or -independent activation of guanine nucleotide-binding proteins by histamine and 2-substituted histamine derivatives in human leukemia (HL-60) and human erythroleukemia (HEL) cells. *Biochem. Pharmacol.* **1995**, *49*, 901–914.
(62) Seifert, R.; Hageluken, A.; Hoer, A.; Hoer, D.; Grunbaum, L.; Offermanns, S.; Schwaner, I.; Zingel, V.; Schunack, W.; Schultz, G. The H_1 receptor agonist 2-(3-chlorophenyl)histamine activates G_i proteins in HL-60 cells through a mechanism that is independent of known histamine receptor subtypes. *Mol. Pharmacol.* **1994**, *45*, 578–586.
(63) Adachi, N.; Liu, K.; Motoki, A.; Nishibori, M.; Arai, T. Suppression of ischemia/reperfusion liver injury by histamine H4 receptor stimulation in rats. *Eur. J. Pharmacol.* **2006**, *544*, 181–187.
(64) Pathak, U.; Raza, S. K.; Kulkarni, A. S.; Vijayaraghvan, R.; Kumar, P.; Jaiswal, D. K. Novel S-substituted aminoalkylamino ethanethiols as potential antidotes against sulfur mustard toxicity. *J. Med. Chem.* **2004**, *47*, 3817–3822.
(65) Hannedouche, J.; Clarkson, G. J.; Wills, M. A new class of "tethered" ruthenium(II) catalyst for asymmetric transfer hydrogenation reactions. *J. Am. Chem. Soc.* **2004**, *126*, 986–987.
(66) Walseth, T. F.; Johnson, R. A. The enzymatic preparation of [α-^{32}P] nucleoside triphosphates, cyclic [^{32}P]AMP, and cyclic [^{32}P]GMP. *Biochim. Biophys. Acta* **1979**, *562*, 11–31.
(67) Cheng, Y.-C.; Prusoff, W. H. Relationship between the inhibition constant (K_I) and the concentration of inhibitor which causes 50% inhibition (I_{50}) of an enzymatic reaction. *Biochem. Pharmacol.* **1973**, *22*, 3099–3108.
(68) Schneider, E. H.; Schnell, D.; Papa, D.; Seifert, R. High constitutive activity and a G-protein-independent high-affinity state of the human histamine H(4)-receptor. *Biochemistry* **2009**, *48*, 1424–1438.
(69) Wang, J.; Wolf, R. M.; Caldwell, J. W.; Kollman, P. A.; Case, D. A. Development and testing of a general amber force field. *J. Comput. Chem.* **2004**, *25*, 1157–1174.
(70) Lovell, S. C.; Word, J. M.; Richardson, J. S.; Richardson, D. C. The penultimate rotamer library. *Proteins* **2000**, *40*, 389–408.
(71) Strasser, A.; Striegl, B.; Wittmann, H. J.; Seifert, R. Pharmacological profile of histaprodifens at four recombinant histamine H-1 receptor species isoforms. *J. Pharmacol. Exp. Ther.* **2008**, *324*, 60–71.
(72) Van der Spoel, D.; Lindahl, E.; Hess, B.; Groenhof, G.; Mark, A. E.; Berendsen, H. J. C. GROMACS: fast, flexible, and free. *J. Comput. Chem.* **2005**, *26*, 1701–1718.
(73) Oostenbrink, C.; Villa, A.; Mark, A. E.; Van Gunsteren, W. F. A biomolecular force field based on the free enthalpy of hydration and solvation: the GROMOS force-field parameter sets 53A5 and 53A6. *J. Comput. Chem.* **2004**, *25*, 1656–1676.
(74) Clark, M.; Cramer, R. D. I.; Van Opdenbosch, N. Validation of the general purpose Tripos 5.2 force field. *J. Comput. Chem.* **1989**, *10*, 982–1012.